TESI DOCTORAL
Paper de l'edema miocardíac en el dany per isquèmia – reperfusió. Estudi de la distribució de l'edema mitjançant ressonància magnètica

Autora: Mireia Andrés Villarreal

Programa de Doctorat: Medicina

Departament de Medicina

Universitat Autònoma de Barcelona

2017

Codirectors

Dr. David Garcia- Dorado

Dr. Ignasi Barba Vert

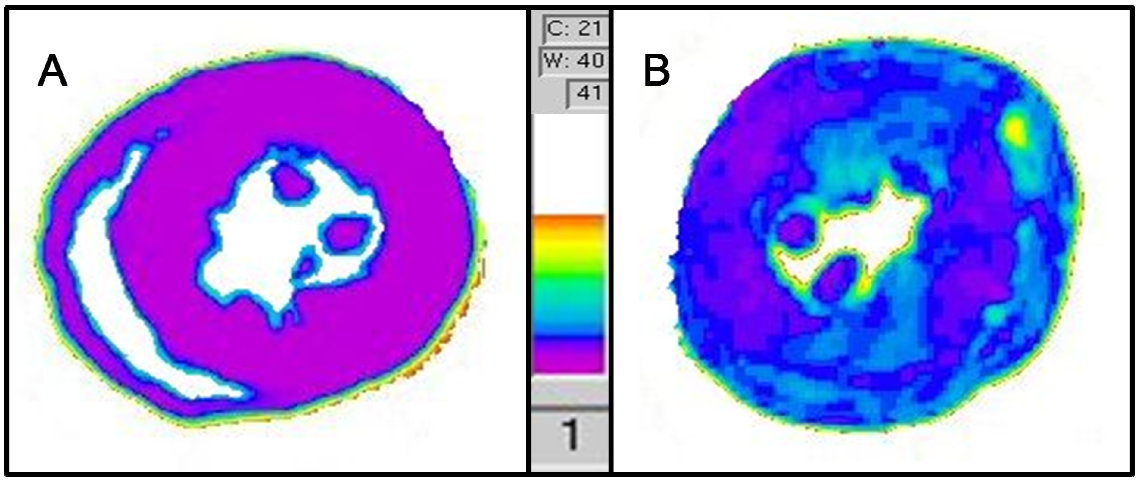

Figura 39: Imatge paramètrica per Relaxació T2: y = A+C *exp(-t/T2). X.A. Imatge corresponent a un tall transversal de cor intacte. X.B. Imatge corresponent a un tall transversal de cor perfós amb tampó normosmòtic durant 40 minuts.

Els valors de T2, densitat protònica i ADC dels grups analitzats estan representats a la taula 5. S'observa un increment significatiu en els valors de T2 i ADC en tots els grups de perfusió salina respecte el cor intacte (i sense diferències significatives entre ells). El valor de densitat protònica és significativament superior respecte el cor intacte als cors perfosos amb tampó normosmòtic i hiposmòtic. En canvi, els cors perfosos amb tampó hiperosmòtic no van presentar un valor significativament diferent de densitat protònica respecte el cor intacte.

	T2 (ms)	ADC (mm^2/s)	DP (%)
Cor intacte	29 ± 3	8 ± 0.9	63 ± 6
Normosmòtic	78 ± 10	13 ± 2	70 ± 4
Hiposmòtic	76 ± 14	13 ±2	73 ± 3
Hiperosmòtic	88 ± 15	14 ± 1,7	66 ± 3

Taula 5. Valors de T2, ADC i DP en els quatre protocols experimentals

Les Figura 40 (A.B.C) mostra els valors (promig i error estàndard) del valor de T2, ADC i DP als quatre grups experimentals: cor intacte, perfusió salina amb tampó normosmòtic, hiposmòtic i hiperosmòtic respectivament. Es pot apreciar l'increment en el valor de T2 i ADC als tres grups de cors perfosos respecte el cor intacte, així com l'increment de DP als cors perfosos amb tampó normosmòtic i hiposmòtic (i no als cors perfosos amb tampó hiperosmòtic)

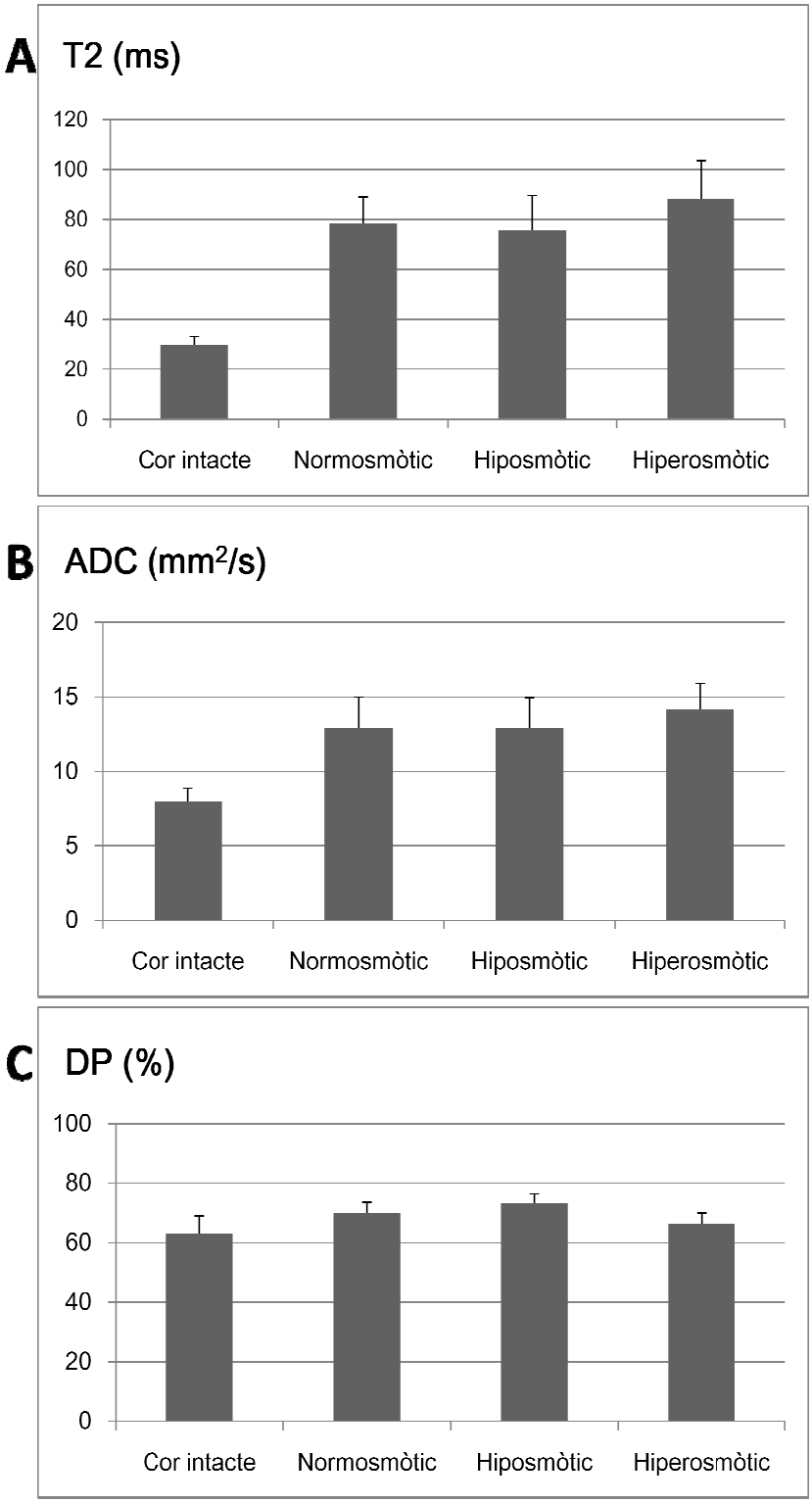

Figura 40. Valors promig i error estàndard de T2 (A), ADC (B) i densitat protònica (DP) als experiments de cor intacte i cor aïllat perfós en situació de normòxia (amb tampó normosmòtic, hiposmòtic i hiperosmòtic).

4.6.3 Relació entre els valors de T2, ADC i DP amb el contingut i la distribució d'aigua

En analitzar la relació de T2 i densitat protònica amb el contingut i la distribució de l'aigua, però, observem com T2 es correlaciona amb el contingut d'aigua extracel·lular ($r^2 = 0.993$, $p < 0.01$) però no amb l'aigua total ($r^2 = 0.305$, p = n.s.), mentre que la densitat protònica es correlaciona de manera lineal amb l'aigua total ($R^2 = 0.988$, $p < 0.01$) i no amb el contingut d'aigua extracel·lular ($r^2 = 0.318$, p = n.s.). El valor del coeficient aparent de difusió (ADC) també es correlaciona amb el contingut d'aigua extracel·lular, tot i que no tan sòlidament com el valor de T2. ($r^2 = 0.893$, $p < 0.01$) [Figura 41].

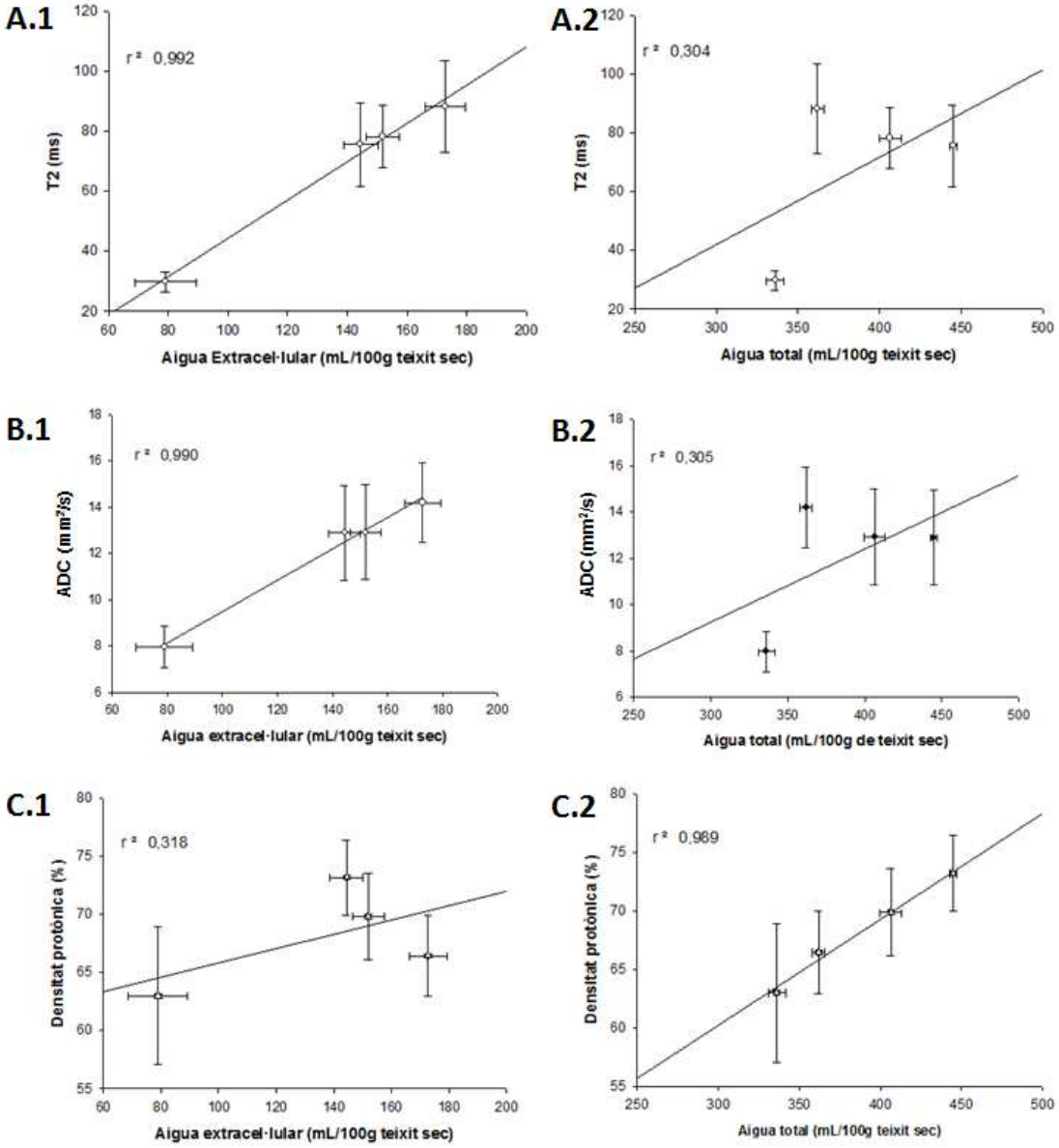

Fig 41. Gràfiques amb la correlació entre T2, ADC i Densitat protònica i el contingut d'aigua extracel·lular i total respectivament. Gràfica A.1. Correlació entre aigua extracel·lular i T2. Gràfica A.2. Correlació entre aigua total i T2. Gràfica B.1. Correlació entre aigua extracel·lular i ADC. Gràfica B.2. Correlació entre aigua total i ADC. Gràfica C.1. Correlació entre aigua extracel·lular i Densitat protònica. Gràfica C.2. Correlació entre aigua total i densitat protònica. A cada gràfica apareix el coeficient de correlació R (regressió lineal, Sigma Plot ®).

4.7 Estudi de RM en pacients

4.7.1 Característiques dels pacients

Es va realitzar estudi de ressonància magnètica cardíaca incloent una seqüència de difusió en dos pacients amb IAMEST i quatre pacients amb discinèsia apical transitòria. Va ser

possible afegir la seqüència de difusió i obtenir una imatge de qualitat adient en els dos pacients amb IAM i en tres dels quatre pacients amb discinèsia apical transitòria. Afegir la seqüència de difusió allarga el temps d'exploració rutinari entre 5 i 10 minuts. Requereix apnees prolongades que no tots els pacients són capaços de mantenir. A continuació es detalla les dades principals d'aquests pacients.

Pacient 1. Home de 74 anys amb IAM anterolateral Killip II. Malaltia de dos vasos: oclusió trombòtica de la descendent anterior proximal i lesió de la interventricular posterior del 70%. Angioplàstia: implant d'stent directe convencional a la DA. Cardio RM realitzada al sisè dia de l'infart: Acinèsia extensa anterior, septal i global apical. Fracció d'ejecció del ventricle esquerre 39% (VTD 121mL i VTS 73mL). Defecte de perfusió en repòs que afecta la cara anterior. Extensa captació transmural als segments anterior basal, mig i apical, anteroseptal mig, septal apical, inferoapical i àpex associat a extens edema miocardíac i hiposenyal suggestiu de transformació hemorràgica.

Pacient 2. Home de 81 anys, hipertens amb IAM inferoposterolateral Killip I. Malaltia d'un vas: oclusió trombòtica de coronària dreta proximal. Angioplàstia: trombectomia i implant d'stent convencional. Cardio RM realitzada al setè dia de l'infart: extensa hipocinèsia inferior basal, mitja i apical. Fracció d'ejecció del ventricle esquerre 57% (VTD 136mL i VTS 57mL). Discret defecte de perfusió en repòs inferior basal i mig amb afectació subendocàrdica (50% del gruix) associat a extens edema miocàrdic.

Pacient 3. Dona de 79 anys, dislipèmica amb discinèsia apical transitòria. Coronariografia: sense lesions coronàries significatives. Cardio RM realitzada al cinquè dia: Acinèsia apical global. Fracció d'ejecció del ventricle esquerre 52% (VTD 57mL/m^2 i VTS 28mL/m^2), associat a edema miocardíac sense defectes de perfusió en repòs després de l'administració de gadolini i sense lesions necròtiques-cicatricials a l'estudi tardà. Recuperació posterior de la fracció d'ejecció del ventricle esquerre fins 78%.

Pacient 4. Dona de 81 anys, hipertensa, diabètica i dislipèmica amb discinèsia apical transitòria. Coronariografia: sense lesions coronàries significatives. Cardio RM realitzada al 12è dia: Dilatació i hipocinèsia apical. Fracció d'ejecció del ventricle esquerre 53% (VTD 85mL i VTS 40mL) associat a edema miocardíac i sense retenció patològica de contrast a l'estudi tardà.

Pacient 5. Dona de 75 anys, hipertensa amb discinèsia apical transitòria. Coronariografia: sense lesions coronàries significatives. Cardio RM realitzada al 8è dia: hipocinèsia anterior i

apical associada a edema miocardíac. Fracció d'ejecció del ventricle esquerre 58% (VTD 98mL i VTS 41mL). Sense retenció patològica de contrast a l'estudi tardà.

Pacient 6. Dona de 77 anyshipertensa, diabètica i dislipèmica amb discinèsia apical transitòria. Coronariografia: sense lesions coronàries significatives. Cardio RM realitzada al 10è dia: Lleu hipocinèsia apical associada a edema miocardíac. Fracció d'ejecció del ventricle esquerre 47% (VTD 103mL i VTS 55mL). Sense retenció patològica de contrast a l'estudi tardà.

Pacient 7. Home de 80 anys, exfumador, hipertens amb IAM inferoposterior Killip II. Malaltia coronària de tres vasos: angioplàstia primària a la CD mitja (oclusió aguda) i angioplàstia diferida a la DA proximal. Cardio RM realitzada al dia 11 després de l'IAM: Fracció d'ejecció del ventricle esquerre 52% (VTD 112 mL i VTS 51 mL). Necrosi no transmural septo-inferior basal i inferior basal i mitja amb criteris de viabilitat. Les seqüències STIR (potenciade sen T2) mostren hiperintensitat de senyal a nivel septo-inferior basal i inferior basal i mig. S'intenta adquirir una seqüència de densitat protònica.

4.7.2 Resultats de l'estudi de ressonància magnètica cardíaca en pacients

Tant els pacients amb infart agut de miocardi amb elevació de l'ST com els pacients amb discinèsia apical transitòria van presentar increment de l'ADC coincident amb les regions d'hiper intensitat de senyal potenciat amb T2 [Figura 42]. Aquesta regió es correspon amb el miocardi discinètic en el cas dels pacients amb discinèsia apical transitòria. Els pacients amb IAMEST a més, presentaven necrosi definida com hiperintensitat del senyal després de l'administració de gadolini, troballa que no es va donar als pacients amb discinèsia apical transitòria.

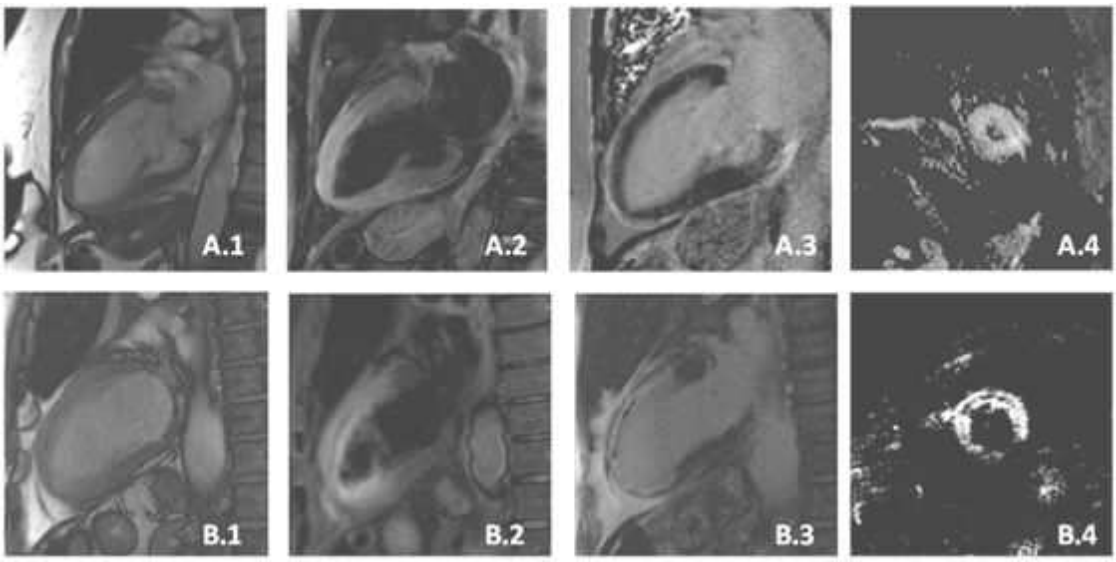

Figura 42. Estudi de cardio RM d'una pacient amb discinèsia apical transitòria (A: primera fila) i d'un pacient amb IAMEST anterior (segona fila: B). La primera columna (A.1 i B.1) es correspon a una imatge en telesístole de les seqüències de cine. La segona (A.2 i B.2) a l'estudi de T2 per detectar edema miocardíac. La tercera columna (A.3 i B.3)pertany a la seqüència de potenciada en T1 per detectar retenció tardana de contrast i la darrera imatge (A.4 i B.4) és l'estudi de difusió. L'estudi tardà després de l'administració de gadolini mostra retenció patològica (necrosi) en el pacient amb IAM però no pas en la pacient amb discinèsia apical transitòria. Les imatges de difusió mostren increment del senyal coincident amb els segments que presentaven increment del senyal en T2 (edema miocardíac). Es pot apreciar com en ambdós casos hi ha important edema miocardíac als segments discinètics.

Adquisició d'imatges de densitat protònica en pacients: L'adquisició d'imatges per valorar densitat protònica, amb temps d'eco llargs (10") que requereixen apnees prolongades, ha proporcionat imatges de qualitat subòptima que no tenen en aquests moments viabilitat per a generalitzar la seva adquisició en estudis clínics, ni tans sols amb finalitat experimental. La Fig 43.A mostra la imatge de densitat protònica obtinguda i la Fig 43.B és la imatge d'un dels talls adquirits després de l'administració de gadolini i mostra la necrosi inferior (hiperintensitat de senyal, fletxa negra)

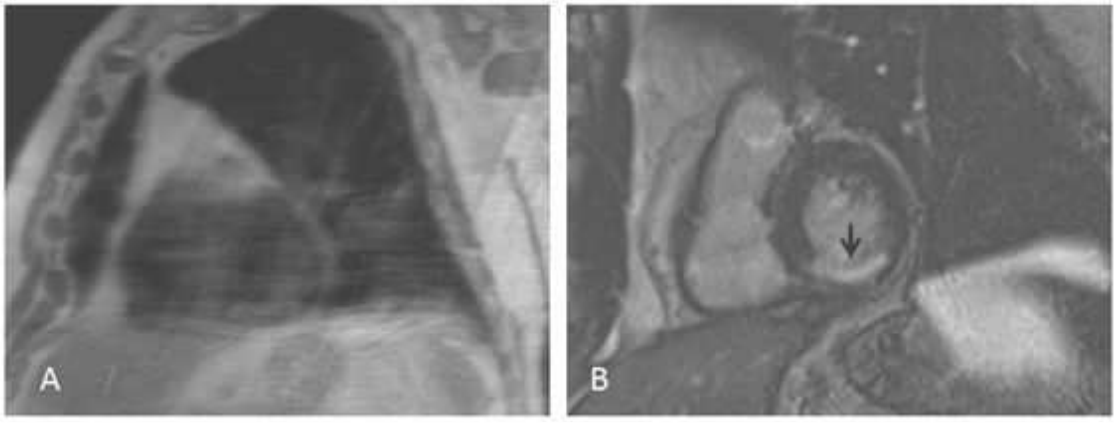

Figura 43. Imatge de densitat protònica (A) i de retenció tardana de gadolini (B) en un pacient amb IAM inferoposterior. Es pot apreciar la pèssima qualitat de la imatge de densitat protònica (A) i la hiperintensitat de senyal corresponent a la retenció tardana de contrast (fletxa), corresponent a la zona de necrosi (B).

5 Discussió

En aquest treball hem posat apunt una tècnica basada en la ressonància magnètica que permet estudiar l'edema i la distribució de l'aigua entre els espais intra i extra-cel·lulars del miocardi. Això ens ha permès demostrar que l'edema és responsable, almenys en part, de la mort per isquèmia / repefusió.

També hem estudiat com diferents paràmetres de les imatges de RM (T1, T2, ADC, DP) correlacionen amb la distribució de l'edema i, finalment, hem realitzat un estudi pilot per avaluar si aquests conceptes es podrien aplicar a la clínica.

5.1 Protocols Experimentals

Per poder estudiar l'edema hem desenvolupat un model experimental basat en la distribució de Gd-DOTA que ens ha permès analitzar l'edema i la distribució de l'aigua en el cor. Aquest model s'ha validat comparant els resultats obtinguts en cor intacte amb dades de la literatura i observant que no hi ha diferències [139]. El mètode es basa en estudiar la distribució de quelats de gadolini que, per motius de grandària, només poden estar en compartiments determinats; aquesta aproximació ja s'havia emprat amb anterioritat marcant els traçadors amb radioactivitat [145]. El mètode que hem desenvolupat té l'avantatge que no utilitza compostos radioactius i, sobretot, que el traçador és d'ús clínic comú, obrint la porta a una possible aplicació clínica.

Les dades prèvies de la literatura queden recollides a la revisió d'Aliev et al [139]: afirmen com a valor més probable de contingut d'aigua intracel·lular 615mL d'aigua per Kg de teixit fresc (que equival a 291mL d'aigua per 100 grams de teixit sec) i de contingut d'aigua extracel·lular 174mL/kg de teixit fresc (que equival a 82mL d'aigua per 100g de teixit sec. Els nostres experiments en cor intacte aporten uns valors molt pròxims a aquests: exactament de 257mL d'aigua intracel·lular i 79mL d'aigua extracel·lular per cada 100g de teixit sec. Tot i que una comparació estadística vàlida no pot ser realitzada, creiem que la proximitat d'aquests valors reforça la validesa i la utilitat del nostre mètode. També cal tenir en compte que no hi ha cap mètode de referència validat que es pugui emprar com a *gold standard*.

5.2 Rellevància de la metodologia desenvolupada

La metodologia més emprada en la quantificació d'espais hídrics (intravascular, intersticial o intracel·lular) està basada en la utilització de radioisòtops. El punt clau és que cal emprar marcadors quantificables amb cinètiques de distribució adients. En aquest sentit, l'ús de radioisòtops suposa l'avantatge que permet marcar pràcticament qualsevol estructura (una molècula de major o menor complexitat o fins i tot cèl·lules) de manera que es pot seleccionar l'estructura més adient per actuar com a marcador d'espai. Aquest mètode té l'inconvenient fonamental de produir radiació gamma, potencialment nociva per la salut. A més, requereix disposar de comptadors gamma entre les instal·lacions i també condiciona i restringeix la metodologia de treball, perquè l'activitat radioactiva minva exponencialment amb el temps i per tant esdevé crucial realitzar les mesures en temps molt precisos i constants en tots els experiments.

La metodologia descrita en aquest estudi suposa l'avantatge de no produir radiacions nocives per la salut i també que el marcador d'espai intersticial emprat no perd activitat en el temps, sinó que la seva presència és inalterable (ja que es tracta d'una espècie química estable, el gadolini). L'estabilitat del marcador, a part de permetre una major flexibilitat en els temps de mesura (cosa que facilita l'organització dels procediments experimentals) permet, per exemple, que estudis realitzats en un centre de recerca puguin enviar les seves mostres a un altre centre que disposi de les instal·lacions de ressonància magnètica per realitzar la mesura. Un inconvenient és que els compostos de gadolini no tenen tanta versatilitat per adaptar-se a marcadors d'espais com la que ofereixen els radioisòtops. Tot i que no han estat emprats en

aquest treball, hi ha disponibles comercialment (o es poden preparar) formulacions de gadolini unit a albúmina que es podria utilitzar com marcador d'espai intravascular.

Per altra banda, avui en dia, l'estudi de l'edema al miocardi es basa fonamentalment en la informació obtenida mitjaçant imatges de ressonància magnètica, de manera que els grups dedicats a aquesta qüestió solen disposar d'aquesta tecnologia, cosa que afegeix valor i utilitat pràctica al mètode.

5.3 Importància de les troballes respecte el paper de l'edema en el dany per isquèmia reperfusió al miocardi

La presència d'edema a l'IAM és coneguda des de fa molts anys [73]; tot i així el seu paper en el dany per isquèmia reperfusió no està clar. Fins ara la majoria d'autors han considerat la seva presència únicament com a marcador de miocardi en risc [146–148]. Les dades proporcionades per aquest treball aporten evidència a favor de la contribució de l'edema miocardíac a la mort dels cardiomiòcits en el context del dany per isquèmia reperfusió, ja que s'ha observat que la reducció de l'edema miocardíac intracel·lular emprant medi de perfusió hiperosmòtic redueix la necrosi.

Estudis previs que correlacionaven edema i mort cel·lular [135] estudiaven l'increment d'aigua total; s'ha de tenir en compte que l'edema miocardíac causat per la necrosi és fonamentalment extracel·lular i és la suma del contingut hídric de les cèl·lules mortes, que perden la integritat del sarcolema i del guany net en contingut d'aigua que es produeix a conseqüència de la presència dels detritus cel·lulars osmòticament actius, de la reacció inflamatòria i del dany vascular amb pèrdua d'integritat endotelial. En augmentar la pressió osmòtica del medi de perfusió, el sarcolema és menys susceptible de perdre la integritat durant la reperfusió. Després dels estudis que correlacionaven l'edema amb la mort cel·lular [73], alguns autors van intentar aplicar aquest fenomen a la clínica en la reducció de l'infart, però aquest efecte no ha demostrat de manera sòlida la seva utilitat com a diana terapèutica [68,150–153]. Les dades obtingudes en aquesta tesi suggereixen que la diana terapèutica hauria de ser de mode específic l'edema intracel·lular i no l'edema total.

L'estudi d'imatge en el model animal ens ha permès estudiar com varien els paràmetres de relaxació (T1 i T2), difusió i quantitat d'aigua en les diferents condicions d'edema i distribució d'aigua que ens permetia el model de cor sotmès a perfusió salina. D'aquesta manera s'ha

observat que els valors de T2 correlacionen molt estretament amb la quantitat d'aigua extracel·lular present al teixit. Aquest resultat entra en contradicció amb la majoria d'estudis previs que descriuen que, en el context de l'IAM, T2 correlaciona amb l'edema total[154,155].

En el cas de la difusió, les nostres dades experimentals en el model de Langendorff també mostren mostren una alta correlació amb l'edema extracel·lular, un comportament molt semblant a T2, de manera que la previsió és trobar increment del senyal de ADC allà on hi hagi increment del senyal de T2, en el cor. Les dades clíniques obtingudes han corroborat aquesta troballa ja que, tant en pacients amb IAM com amb DAT s'observa un increment del senyal de ADC allà on hi ha increment del senyal de T2. Es va triar la seqüència de difusió perquè estudis previs de ressonància magnètica en cervell en el context de l'ictus mostraven una correlació de la ADC amb l'aigua extracel·lular i aporta detalls rellevants que ajuden a establir com d'evolucionat està el dany cerebral [156,157]. Les dades del present treball, però, no corroboren aquest comportament de les seqüències de difusió en el cor.

La densitat protònica mesura la quantitat d'hidrògens presents en un volum determinat independentment del seu entorn ja que no es tenen en compte els efectes de la relaxació. Com era d'esperar les imatges de DP correlacionen amb la quantitat total d'aigua. Per obtenir imatges de densitat protònica cal emprar temps entre polsos (TR) molt llargs (idealment 5*T1); si bé és senzill en els cors aïllats i estàtics, és inviable avui en dia en estudis amb pacients. A més, per poder quantificar els hidrògens caldria obtenir imatges amb TE = 0, cosa que és físicament impossible. En aquest treball hem pogut obtenir aplicar una seqüència per intentar estimar el valor de DP en pacients adquirint cada 3 batecs cardíacs amb resultats poc satisfactoris. Si en un futur els avenços en l'electrònica i seqüències de polsos permeten estimar DP en un únic cicle cardíac els estudis de DP serien aplicables en la pràctica clínica diària.

L'evidència proporcionada pel present estudi suggereix que l'increment de senyal de T2 es correlaciona específicament amb l'aigua extracel·lular i no amb l'aigua total. Tot i que ho podria semblar, aquesta afirmació no entra en contradicció amb tota l'evidència de correlació de T2 amb l'edema total. Les situacions clíniques que cursen amb important edema miocardíac i per tant, amb increment del senyal de T2 a l'estudi de ressonància magnètica cardíaca, es caracteritzen justament per edema a expenses de la fracció extracel·lular. El fet que no s'hagi trobat fins el moment una situació clínica real que cursi amb edema miocardíac a expenses fonamentalment d'edema intracel·lular fa que a la pràctica, la correlació de T2 amb l'edema en general, és a dir, amb l'aigua total, sigui ben certa. En base als nostres resultats, seria

esperable que si aquesta situació clínica es produís, l'estudi de ressonància magnètica mostrés escàs increment del senyal potenciat en T2 als segments amb edema intracel·lular. Si bé aquesta situació és una mera especulació, les dades obtingudes permeten induir que a la discinèsia apical transitòria, caracteritzada a l'estudi de ressonància magnètica com increment del senyal potenciat en T2 als segments discinètics, en absència necrosi significativa, hi predomina un important edema extracel·lular que no és atribuïble a la ruptura del sarcolema. Aquest detall obre la porta a generar noves hipòtesis en relació a una situació clínica envoltada encara de molts interrogants i suggereix l'alteració de la permeabilitat vascular com un possible mecanisme implicat en la fisiopatologia de la discinèsia apical transitòria.

A la llum de l'evidència aportada amb el present treball en quant a la rellevància de la distribució de l'edema i no només a la quantitat total d'edema al miocardi, sembla raonable continuar investigant per tal de fer possible analitzar clínicament la distribució de l'edema. És possible que les seqüències de mapes de T1 adquirides després de l'adminsitració de gadolini puguin contribuir a aquesta valoració. Seria convenient que els estudis dirigits a valorar l'impacte d'estratègies per reduir l'extensió de l'infart incloguessin als estudis de cardioressonància magnètica no només seqüències potenciades en T2 per valorar edema total i de retenció tardana de Gd per quantificar la necrosi, sinó alguna seqüència prèviament validada per establir la distribució de l'edema al miocardi. També seria molt interessant, en la línia dels treballs de Fernandez-Jimenez et al[158], establir el patró al llarg dels primers dies postinfart de la distribució de l'edema al miocardi, per adquirir un major coneixement fisiopatològic de l'edema que pugui donar peu a proposar possibles intervencions terapèutiques dirigides a reduir l'extensió de l'infart.

Un cop demostrat que tant l'increment de senyal potenciat en T2 com l'ADC reflecteixen edema extracel·lular, convindria posar a punt noves seqüències dirigides a valorar l'edema total o l'edema intracel·lular. Un punt feble d'aquest treball és el fet de no haver trobat una seqüència aplicable clínicament per quantificar o semiquantificar l'edema total o intracel·lular. També és un punt feble el fet de disposar de cap model (ni experimental ni clínic) caracteritzat per edema intracel·lular pur, en absència d'edema extracel·lular significatiu. El fet de no disposar d'aquest model hipotètic dificulta valorar la utilitat de seqüències que podrien ser útils per valorar edema intracel·lular. Per altra banda, el fet que clínicament no hi hagi situacions descrites d'edema intracel·lular pur o predominant, qüestiona la utilitat d'un hipotètic model

experimental d'aquestes característiques, ja que no tindria traslació clínica. Tindria únicament el sentit d'ajudar a definir millor el significat de determinades seqüències de cardioressonància magnètica dirigides a l'estudi de l'edema.

La reperfusió amb medi hiperosmòtic ha estat posada a prova de forma repetida per la seva potencial utilitat per reduir l'extensió de l'infart i s'ha provat efectiva en la protecció del cor amb cardioplexia en el context de la cirurgia cardíaca [150,152,159,160]. Les dades experimentals aporten evidència de la influència de l'edema sobre la mort cel·lular en el context del dany per isquèmia reperfusió, encara que per ara no s'ha trobat la manera de reduir l'extensió de l'infart en pacients tot actuant sobre aquesta diana en el context de l'infart agut de miocardi.

Detectem i quantifiquem la necrosi tot mesurant la quantitat de LDH, un enzim intracel·lular que s'allibera al medi extern quan té lloc la ruptura del sarcolema. Per tant, una cèl·lula irreversiblement danyada però que encara preserva la integritat del sarcolema, no seria identificada per aquest mètode ni per cap altre basat en la detecció d'enzims intracel·lulars miocardíacs (creatin cinasa o troponines). Les dades indueixen a no descartar l'edema miocardíac com a possible diana terapèutica, malgrat la dificultat que suposa intervenir per controlar l'edema del miocardi durant la reperfusió en un context clínic.

Una part important del present treball ha estat realitzat fonamentalment en un model de cor de rata aïllat sotmès a perfusió salina. Aquesta aproximació ens ha permès crear models amb diferent distribució d'aigua entre compartiments ajustant la composició del medi de perfusió i amb la prevenció de la ruptura del sarcolema amb blebbistastina. Aquesta estratègia no està prèviament descrita a la literatura científica. Tot i així el model presenta limitacions que no es poden obviar, la principal és que la perfusió en sí mateixa provoca edema i això impossibilita obtenir edema intracel·lular pur, és a dir, en absència d'edema intersticial rellevant.

5.4 Impacte de les troballes als estudis en pacients

La caracterització de l'edema miocardíac s'ha basat des dels anys 1990 en l'increment de senyal a les seqüències potenciades en T2 [7,73,141,146,147]. És molt abundant a la literatura l'evidència a favor de la correlació de l'increment del senyal de T2 amb l'edema al miocardi. Si bé en el context de l'infart agut de miocardi s'ha acceptat també la correlació de l'àrea amb increment de senyal potenciat en T2 amb el miocardi en risc, a l'actualitat aquest concepte és controvertit [81,146]. Fins que aquesta correlació estigui millor definida, seria prudent no emprar la

l'estimació de l'àrea en risc per aquest mètode com a part de la mesura de la reducció de l'extensió de l'infart als assaigs clínics

A la darrera dècada també s'ha anat desenvolupant la tecnologia per adquirir mapes de T1 al miocardi (exposat o no a l'admistració de gadolini)[85,86,161–164]. Els mapes de T1 adquirits durant l'administració de gadolini donen informació sobre el volum extracel·lular del miocardi i per tant, també proporcionen informació rellevant en quant a la distribució de l'edema al miocardi. Tot i que aquestes seqüències no s'han desenvolupat amb aquesta finalitat, sinó més aviat amb l'interés de caracteritzar millor miocardipoaties que cursen amb fibrosi difusa que queda mal definida amb els estudis rutinaris de retenció tardana de contrast, els mapes de T1 sense gadolini han demostrat la seva validesa per definir el miocardi en risc definit com l'àrea d'increment de senyal de T2[87,165,166]. En el present treball no s'ha emprat aquesta metodologia perquè no estava disponible clínicament. En qualsevol cas, els mapes de T1 reflecteixen novament espai extracel·lular. Continua, per tant, havent el buit de seqüències dedicades a la quantificació d'edema total o intracel·lular.

En aquesta tesi s'ha dut a terme un estudi pilot en pacients per comprovar la possible translacionalitat dels resultats obtinguts al laboratori.

S'ha focalitzat l'estudi clínic en el context de la síndrome coronària aguda, concretament en l'infart agut de miocardi i la discinèsia apical transitòria. Aquestes dues situacions clíniques tenen similituds i diferències que fan interessant el seu estudi comparatiu mitjançant ressonància magnètica. La presentació clínica típica en els dos escenaris és habitualment indiferenciable: es caracteritza per dolor toràcic anginós i elevació del segment ST a l'electrocardiograma, suggestiu d'IAM amb elevació de l'ST i per tant amb sospita d'oclusió coronària aguda. L'actuació inicial, per tant, consisteix en realitzar una coronariografia immediata. En el cas d'infart agut de miocardi se sol trobar malaltia coronària aguda que justifica el quadre clínic però en canvi, en el cas de la discinèsia apical transitòria no hi ha lesions coronàries angiogràficament significatives. Tot i així, a la fase aguda de la discinèsia apical transitòria es documenten transtorns de la motilitat segmentària miocàrdica similars a l'IAM i l'estudi de ressonància magnètica sol documentar, tant a l'IAM com a la discinèsia apical transitòria, increment del senyal el T2 al miocardi en risc o al miocardi discinètic respectivament. La diferència fonamental rau en què els IAM cursen amb necrosi significativa (tant mesurada de enzimàticament com a l'estudi de ressonància magnètica, identificada com les zones amb retenció tardana de gadolini) mentre que la discinèsia apical transitòria cursa

amb discreta elevació d'enzims i sense necrosi significativa a l'estudi de ressonància magnètica. A més, la discinèsia apical transitòria, com el seu nom indica, és reversible i la motilitat del miocardi es normalitza en poques setmanes. Des del punt de vista de l'estudi de ressonància magnètica trobem dos models d'important edema miocardíac, un amb necrosi significativa i l'altre sense ella. Per això hem cregut interessant aprofundir en l'estudi de l'edema miocardíac en aquests dos models d'edema, amb i sense necrosi, amb la hipòtesi de partida de trobar diferències en els patrons de les seqüències analitzades dirigides a avaluar la distribució de l'edema miocardíac.

En 6 pacients s'ha pogut afegir seqüències de difusió al protocol clínic estàndard. La realització d'aquestes seqüències requereix la col·laboració i capacitat del pacient, calen apnees més prolongades que per la resta de seqüències i implica també allargar el temps d'exploració.

El fet de constatar que les zones d'increment de senyal de difusió se superposen amb les zones d'increment de senyal en T2 juntament amb la dificultat tècnica i pitjor ressolució de les imatges pesades en difusió fa que una possible aplicació clínica de les imatges de difusió depengui del desenvolupament de noves i més ràpides seqüències de polsos.

L'estudi realitzat amb imatges de ressonància magnètica, tant experimental com les exploracions realitzades a pacients com a "prova de concepte" suggereixen que l'increment del senyal en T2 es correspon amb l'increment d'aigua extracel·lular. Si bé aquest detall aporta poc valor afegit en el context de l'infart agut de miocardi (que cursa amb ruptura de sarcolema), és altament rellevant en el context de la discinèsia apical transitòria, la fisiopatologia de la qual encara és poc coneguda. Poder afirmar que l'edema miocardíac en aquest context és fonamentalment extracel·lular suggereix alguns mecanismes implicats com podria ser l'alteració en la permeabilitat vascular.

Malgrat l'escàs nombre de pacients a qui s'ha realitzat la seqüència de difusió en l'estudi de ressonància magnètica cardíaca, aquesta prova de concepte ha pogut validar plenament les dades experimentals obtingudes en el model de cor de rata sotmès a perfusió salina. Una de les principals limitacions de l'estudi ha estat que per poder realitzar la la seqüència de difusió aplicada a l'estudi del cor requereix la col·laboració i capacitat del pacient: cal apnees més prolongades que per la resta de seqüències i la resolució espacial de la seqüència és menor. Incloure una seqüència adicional al protocol implica també allargar el temps d'exploració. Per aquest motiu no s'ha pogut aplicar a tots els pacients que havien donat el seu consentiment

informat. Hi ha hagut pacients que no han estat capaços de realitzar l'apnea necessària com per obtenir imatges de qualitat suficient. Cal tenir en compte que es tracta de pacients d'edat avançada i amb una síndrome coronària aguda recent.

L'estudi de densitat protònica en aquests moments no té viabilitat clínica perquè exigeix un temps de eco molt prolongat (durant 3 cicles cardíacs) i la imatge obtinguda no té resolució espacial ni nitidesa suficient per generar estudis de qualitat suficient. En el futur es podria valorar si les seqüències de mapes de T1 es poden ajustar per obtenir semiquantificacions d'espai intersticial que pugui reflectir en el context clínic adient una mesura d'edema extracel·lular.

5.5 Consideracions metodològiques

5.5.1 Unitats emprades per expressar el contingut d'aigua en els diferents compartiments

A la literatura científica sobre edema miocardíac trobem diverses maneres d'expressar la quantitat d'aigua present als teixits. Bàsicament es pot expressar en percentatge de la quantitat d'aigua respecte el pes total de la mostra o bé referida a la quantitat d'aigua respexte el pes sec [139,149]. Tot i que la informació sotsjacent és la mateixa i és igualment correcta independentment de la forma de presentar les dades, l'experiència que ens proporciona aquest treball fa considerar que la millor manera de presentar les dades és respecte al pes sec.

Quan s'expressa en percentatge (respecte el pes total de la mostra) indueix fàcilment a errors d'interpretació dels resultats. Això és així perquè en referir el contingut d'aigua (total o compartimental) al pes total de la mostra, la variable "aigua total" queda inclosa al denominador. Això pot portar en determinades circumstàncies al fet que petits increments en el contingut d'aigua d'un dels compartiments, en el context d'un increment molt més notable de l'altre compartiment, quedi reflectit com un descens en el percentatge d'aigua [Figura 43 i Taula 6]. Per aquest motiu nosaltres recomanem referir el contingut d'aigua al pes sec de la mostra.

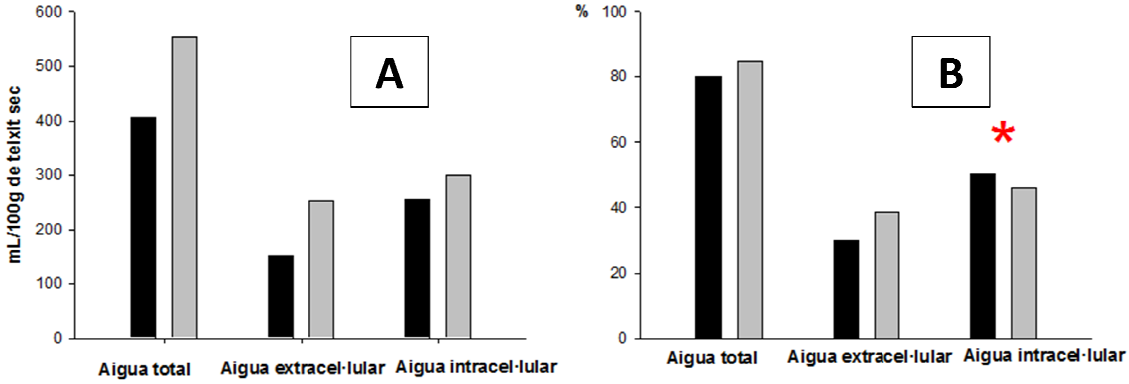

Figura 43. Exemple gràfic de com les unitats emprades per expressar els resultats pot confondre alhora d'interpretar les dades. La gràfica A. mostra el contingut d'aigua (total, extracel·lular i intracel·lular) com mL d'aigua sobre el teixit sec, mentre que la gràfica B expressa la mateixa informació però en forma de percentatge sobre el teixit fresc. Estan exemplificats dos experiments hipotètics diferents: Experiment 1 (barres negres) i Experiment 2 (barres grises). Es pot apreciar com el contingut d'aigua intracel·lular, que en realitat és superior a l'experiment 2, a la gràfica B (percentatge) aparenta com menor respecte l'experiment 1 (*). Això és degut al fet que en expressar les dades com a percentatge i no de manera absoluta, els increments absoluts proporcionalment petits esdevenen disminucions relatives.

Taula 6. Expressió numèrica de les dades expressades a la Figura 43.

	Experiment hipotètic 1		Experiment hipotètic 2	
Aigua total	406 mL/100g teixit sec	80 %	553 mL/100g teixit sec	84 %
Aigua EC	152 mL/100g teixit sec	30 %	253 mL/100g teixit sec	38 %
Aigua IC	254 mL/100g teixit sec	50 %	300 mL/100g teixit sec	46 %

Del mateix mode, a tall d'exemple, les dades aportades a la revisió d'Aliev et al [139], el contingut d'aigua s'expressa en volum d'aigua en relació al pes fresc de la mostra. Així, afirmen que el contingut més probable d'aigua intracel·lular és de 615mL/Kg de teixit fresc, el contingut de massa seca intracel·lular de 189g/Kg de teixit fresc, el contingut d'aigua extracel·lular és de 174mL/Kg de teixit fresc i el de massa seca extracel·lular de 22g/Kg de teixit fresc. Si volem convertir aquestes unitats a mL d'aigua per massa de teixit sec, cal sumar els pesos de teixit sec (189 + 22 = 211g) i referir a aquesta massa els volums d'aigua: 615mL/211g * 100 = 291mL d'aigua intracel·lular per cada 100g de teixit sec i 174mL/211g*100 = 82mL d'aigua extracel·lular. La massa seca de la mostra no varia al llarg de l'experiment, però la massa fresca variarà en funció del grau d'edema ocasionat. Per aquest motiu és essencial referir els continguts d'aigua a una massa de referència estable que no variï amb la variable d'estudi (el contingut d'aigua).

5.5.2 Manipulació de la mostra

Les dades de la literatura que estudien l'edema en el model de cor aïllat sotmès a perfusió salina ofereixen una gran variabilitat en els valors totals i la distribució d'aigua. Part d'aquesta important variació pot ser deguda a diferents maneres de processar les mostres. En primer lloc, en retirar els cors del sistema de perfusió hi queda una quantitat considerable de tampó de perfusió (tant envoltant el cor com a l'interior de les cavitats cardíaques). Si no es vol sobreestimar el contingut d'aigua extracel·lular, cal retirar amb cura aquestes restes de tampó. Per altra banda, un excés d'assecat pot causar infra estimació del contingut d'aigua extracel·lular. Sota el nostre punt de vista aquest punt és crític per tal d'obtenir resultats vàlids i reproduibles. Els protocols emprats s'han estandaritzat per reduir variabilitat: s'ha procurat retirar aquest excés d'aigua present a les mostres tot manipulant-les sobre plaques de plàstic i membranes de niló, enlloc de paper secant de laboratori per evitar retirar una excessiva quantitat d'aigua per fenomen de capil·laritat; a més s'ha realitzat una centrifugació suau sobre la membrana de niló per tal de retirar l'aigua sobrera. Aquesta tècnica garanteix control i homogeneïtat alhora de manipular les mostres, de manera que el grau d'eliminació de l'aigua sobrera sigui similar. És important estandaritzar aquest pas en els estudis d'edema en model de cor aïllat sotmès a perfusió salina; considerem que el mètode presentat en aquesta tesi pot ser un bon punt de partida per assolir aquest objectiu.

Un altre aspecte a considerar pel que fa la manipulació de la mostra afecta al nombre d'extractes necessaris per tal d'obtenir una recuperació adient del quelat de gadolini. Aquest és el pas que es realitza sobre la mostra un cop liofilitzada i micronitzada. Si el contingut de gadolini de la mostra és elevat convé realitzar més d'un extracte per garantir una obtenció completa del gadolini. Cada extracte addicional, però, implica una nova manipulació de la mostra i per tant, la possibilitat d'afegir error a la mesura. Convé fer proves pilot dirigides a establir la dosi de gadolini que convé administrar per tal que les mostres tinguin un contingut de gadolini dintre d'un rang adient i també optimitzar el mètode d'extracció per procurar haver de fer el menor nombre possible d'extraccions.

6 Resum de resultats

En aquest treball s'ha desenvolupat un mètode basat en la utilització de quelats de gadolini com marcadors d'espai extracel·lular per analitzar la distribució de l'aigua al miocardi en el model de cor de rata tant *in vivo* com aïllat i sotmès a perfusió salina.

El recurs d'emprar tampons de perfusió amb diferents osmolaritats permet generar models de cor de rata aïllat amb graus variables d'edema total i amb patrons diferenciats en quant a la distribució de l'edema entre els espais intracel·lular i extracel·lular: la perfusió salina isotònica ja causa per ella mateixa un important edema intersticial. La perfusió amb tampó hiposmòtic s'acompanya d'un increment addicional de l'espai intracel·lular. En canvi, la perfusió amb tampó hiperosmòtic enriquit amb manitol accentua discretament l'increment de l'espai intersticial mentre que redueix el contingut d'aigua intracel·lular.

L'estudi d'imatge amb ressonància magnètica en el cor aïllat de rata amb seqüències potenciades en T2, difusió i densitat protònica permet valorar al grau d'edema total i extracel·lular. La intensificació del senyal del miocardi en seqüències d'imatge potenciades en T2 i en difusió reflecteix l'edema extracel·lular, mentre que el valor relatiu de densitat protònica es correlaciona amb el contingut d'aigua total del miocardi.

Ha estat possible afegir a l'estudi rutinari de ressonància magnètica cardíaca, la seqüència potenciada en difusió a la majoria de pacients en què s'ha proposat l'estudi. No ha estat possible, en canvi, adquirir imatges de qualitat suficient per l'estudi de densitat protònica en pacients. Tant els pacients amb infart agut de miocardi amb elevació de l'ST (IAMEST) com els

pacients amb discinèsia apical transitòria presenten a l'estudi de ressonància magnètica cardíaca realitzat durant la fase aguda (primeres 2 setmanes) un patró d'increment del senyal a les imatges potenciades en T2. Tant els pacients amb IAMEST com els pacients amb discinèsia apical transitòria presenten increment del senyal en les seqüències potenciades en difusió a les regions amb hiperintensitat del senyal a les seqüències potenciades en T2. En base a les dades obtingudes dels estudis experimentals, els patrons dels estudis suggereixen que tant en el cas de l'IAMEST com en el cas de la discinèsia apical transitòria, a la fase aguda hi ha important edema miocardíac a expenses de l'espai extracel·lular.

Els cors perfosos amb tampó hipertònic mostren menor necrosi que els cors control. Així mateix, la reducció de la necrosi durant la reperfusió amb blebbistatina (inhibidor de la hipercontractura), redueix el grau d'edema. Aquests dos fets complementaris suggereixen que l'edema al miocardi associat al dany d'isquèmia reperfusió no és només una conseqüència del dany sinó que contribueix a la necrosi i és, per tant, raonable considerar-lo com una diana terapèutica.

7 Conclusions

El dany per isquèmia reperfusió ocasiona un notable increment del contingut d'aigua del miocardi a expenses del compartiment extracel·lular. En el model de cor de rata aïllat sotmès a perfusió salina, la reducció de la mort cel·lular mitjançant l'administració de blebbistatina a l'inici de la reperfusió redueix l'extensió de l'infart i el grau d'edema del miocardi. Així mateix, controlar l'edema miocardíac durant la reperfusió amb tampons hiperosmòtics, redueix l'extensió de l'infart. Aquestes dades recolzen la hipòtesi que l'edema miocardíac contribueix a la mort cel·lular durant la reperfusió i podria ser considerat com a diana terapèutica en el dany per isquèmia reperfusió.

8 Bibliografia

1. Smith, D., Engel, B., Diskin, A. M., Spanel, P. & Davies, S. J. Comparative measurements of total body water in healthy volunteers by online breath deuterium measurement and other near-subject methods. *Am. J. Clin. Nutr.* **76,** 1295–1301 (2002).
2. Clegg, J. S. Intracellular water and the cytomatrix: some methods of study and current views. *J. Cell Biol.* **99,** 167s–171s (1984).
3. Danziger, J. & Zeidel, M. L. Osmotic homeostasis. *Clin. J. Am. Soc. Nephrol. CJASN* **10,** 852–862 (2015).
4. Michel, C. C. Starling: the formulation of his hypothesis of microvascular fluid exchange and its significance after 100 years. *Exp. Physiol.* **82,** 1–30 (1997).
5. Siddall, E. C. & Radhakrishnan, J. The pathophysiology of edema formation in the nephrotic syndrome. *Kidney Int.* **82,** 635–642 (2012).
6. Hoffmann, E. K., Lambert, I. H. & Pedersen, S. F. Physiology of cell volume regulation in vertebrates. *Physiol. Rev.* **89,** 193–277 (2009).
7. Garcia-Dorado, D. *et al.* Analysis of myocardial oedema by magnetic resonance imaging early after coronary artery occlusion with or without reperfusion. *Cardiovasc. Res.* **27,** 1462–1469 (1993).
8. Hiramitsu, S. *et al.* Transient ventricular wall thickening in acute myocarditis: a serial echocardiographic and histopathologic study. *Jpn. Circ. J.* **65,** 863–866 (2001).
9. Zagrosek, A. *et al.* Relation between myocardial edema and myocardial mass during the acute and convalescent phase of myocarditis--a CMR study. *J. Cardiovasc. Magn. Reson. Off. J. Soc. Cardiovasc. Magn. Reson.* **10,** 19 (2008).
10. Marie, P. Y. *et al.* Detection and prediction of acute heart transplant rejection with the myocardial T2 determination provided by a black-blood magnetic resonance imaging sequence. *J. Am. Coll. Cardiol.* **37,** 825–831 (2001).
11. Sasaguri, S. *et al.* Early detection of cardiac allograft rejection with proton nuclear magnetic resonance. *Circulation* **72,** II231-236 (1985).
12. Davis, K. L., Mehlhorn, U., Laine, G. A. & Allen, S. J. Myocardial edema, left ventricular function, and pulmonary hypertension. *J. Appl. Physiol. Bethesda Md 1985* **78,** 132–137 (1995).
13. Mehlhorn, U., Davis, K. L., Laine, G. A., Geissler, H. J. & Allen, S. J. Myocardial fluid balance in acute hypertension. *Microcirc. N. Y. N 1994* **3,** 371–378 (1996).

14. Dongaonkar, R. M., Stewart, R. H., Geissler, H. J. & Laine, G. A. Myocardial microvascular permeability, interstitial oedema, and compromised cardiac function. *Cardiovasc. Res.* **87,** 331–339 (2010).

15. Luetkens, J. A. *et al.* Comprehensive Cardiac Magnetic Resonance for Short-Term Follow-Up in Acute Myocarditis. *J. Am. Heart Assoc.* **5,** (2016).

16. Raisky, O. *et al.* VEGFR-1 and -2 regulate inflammation, myocardial angiogenesis, and arteriosclerosis in chronically rejecting cardiac allografts. *Arterioscler. Thromb. Vasc. Biol.* **27,** 819–825 (2007).

17. Mehlhorn, U., Geissler, H. J., Laine, G. A. & Allen, S. J. Myocardial fluid balance. *Eur. J. Cardio-Thorac. Surg. Off. J. Eur. Assoc. Cardio-Thorac. Surg.* **20,** 1220–1230 (2001).

18. Levick, J. R. Revision of the Starling principle: new views of tissue fluid balance. *J. Physiol.* **557,** 704 (2004).

19. Laine, G. A. & Granger, H. J. Microvascular, interstitial, and lymphatic interactions in normal heart. *Am. J. Physiol.* **249,** H834-842 (1985).

20. Sun, S. C. & Lie, J. T. Cardiac lymphatic obstruction: ultrastructure of acute-phase myocardial injury in dogs. *Mayo Clin. Proc.* **52,** 785–792 (1977).

21. Mehlhorn, U. *et al.* Impact of cardiopulmonary bypass and cardioplegic arrest on myocardial lymphatic function. *Am. J. Physiol.* **268,** H178-183 (1995).

22. Curry, F.-R. E. & Adamson, R. H. Vascular permeability modulation at the cell, microvessel, or whole organ level: towards closing gaps in our knowledge. *Cardiovasc. Res.* **87,** 218–229 (2010).

23. Ntusi, N. A. B. *et al.* Diffuse Myocardial Fibrosis and Inflammation in Rheumatoid Arthritis: Insights From CMR T1 Mapping. *JACC Cardiovasc. Imaging* **8,** 526–536 (2015).

24. Ntusi, N. A. B. *et al.* Subclinical myocardial inflammation and diffuse fibrosis are common in systemic sclerosis--a clinical study using myocardial T1-mapping and extracellular volume quantification. *J. Cardiovasc. Magn. Reson. Off. J. Soc. Cardiovasc. Magn. Reson.* **16,** 21 (2014).

25. Saeed, M., Hetts, S. W., Jablonowski, R. & Wilson, M. W. Magnetic resonance imaging and multi-detector computed tomography assessment of extracellular compartment in ischemic and non-ischemic myocardial pathologies. *World J. Cardiol.* **6,** 1192–1208 (2014).

26. Kloner, R. A. *et al.* Ultrastructural evidence of microvascular damage and myocardial cell injury after coronary artery occlusion: which comes first? *Circulation* **62,** 945–952 (1980).

27. Mehta, J. L., Nichols, W. W. & Mehta, P. Neutrophils as potential participants in acute myocardial ischemia: relevance to reperfusion. *J. Am. Coll. Cardiol.* **11,** 1309–1316 (1988).

28. Kloner, R. A., Ganote, C. E. & Jennings, R. B. The 'no-reflow' phenomenon after temporary coronary occlusion in the dog. *J. Clin. Invest.* **54,** 1496–1508 (1974).

29. Niccoli, G., Burzotta, F., Galiuto, L. & Crea, F. Myocardial no-reflow in humans. *J. Am. Coll. Cardiol.* **54,** 281–292 (2009).

30. Neumann, F. J. *et al.* Cardiac release of cytokines and inflammatory responses in acute myocardial infarction. *Circulation* **92,** 748–755 (1995).

31. Krejci, J., Mlejnek, D., Sochorova, D. & Nemec, P. Inflammatory Cardiomyopathy: A Current View on the Pathophysiology, Diagnosis, and Treatment. *BioMed Res. Int.* **2016,** 4087632 (2016).

32. Friedrich, M. G. & Marcotte, F. *Cardiac magnetic resonance assessment of myocarditis.* **6,** (2013).

33. Mahrholdt, H. *et al.* Cardiovascular magnetic resonance assessment of human myocarditis: a comparison to histology and molecular pathology. *Circulation* **109,** 1250–1258 (2004).

34. Abdel-Aty, H. *et al.* Diagnostic performance of cardiovascular magnetic resonance in patients with suspected acute myocarditis: comparison of different approaches. *J. Am. Coll. Cardiol.* **45,** 1815–1822 (2005).

35. Hundley, W. G. *et al.* ACCF/ACR/AHA/NASCI/SCMR 2010 expert consensus document on cardiovascular magnetic resonance: a report of the American College of Cardiology Foundation Task Force on Expert Consensus Documents. *J. Am. Coll. Cardiol.* **55,** 2614–2662 (2010).

36. Friedrich, M. G. *et al.* Cardiovascular magnetic resonance in myocarditis: A JACC White Paper. *J. Am. Coll. Cardiol.* **53,** 1475–1487 (2009).

37. Vecchiati, A., Tellatin, S., Angelini, A., Iliceto, S. & Tona, F. Coronary microvasculopathy in heart transplantation: Consequences and therapeutic implications. *World J. Transplant.* **4,** 93–101 (2014).

38. LEAF, A. Maintenance of concentration gradients and regulation of cell volume. *Ann. N. Y. Acad. Sci.* **72,** 396–404 (1959).

39. Inserte, J., Garcia-Dorado, D., Ruiz-Meana, M., Solares, J. & Soler, J. The role of Na+-H+ exchange occurring during hypoxia in the genesis of reoxygenation-induced myocardial oedema. *J. Mol. Cell. Cardiol.* **29,** 1167–1175 (1997).

40. Piper, H. M., Garcia-Dorado, D. & Ovize, M. A fresh look at reperfusion injury. *Cardiovasc. Res.* **38,** 291–300 (1998).

41. Garcia-Dorado, D., Andres-Villarreal, M., Ruiz-Meana, M., Inserte, J. & Barba, I. Myocardial edema: a translational view. *J. Mol. Cell. Cardiol.* **52,** 931–939 (2012).

42. Vandenberg, J. I., Rees, S. A., Wright, A. R. & Powell, T. Cell swelling and ion transport pathways in cardiac myocytes. *Cardiovasc. Res.* **32,** 85–97 (1996).

43. Tritto, F. P., Inserte, J., Garcia-Dorado, D., Ruiz-Meana, M. & Soler-Soler, J. Sodium/hydrogen exchanger inhibition reduces myocardial reperfusion edema after normothermic cardioplegia. *J. Thorac. Cardiovasc. Surg.* **115,** 709–715 (1998).

44. Hoffmann, E. K., Lambert, I. H. & Pedersen, S. F. Physiology of cell volume regulation in vertebrates. *Physiol. Rev.* **89,** 193–277 (2009).

45. Klein, H. H., Pich, S., Bohle, R. M., Wollenweber, J. & Nebendahl, K. Myocardial protection by Na(+)-H+ exchange inhibition in ischemic, reperfused porcine hearts. *Circulation* **92,** 912–917 (1995).

46. Quist, A. P., Rhee, S. K., Lin, H. & Lal, R. Physiological role of gap-junctional hemichannels. Extracellular calcium-dependent isosmotic volume regulation. *J. Cell Biol.* **148,** 1063–1074 (2000).

47. Li, L., Weng, Z., Yao, C., Song, Y. & Ma, T. Aquaporin-1 Deficiency Protects Against Myocardial Infarction by Reducing Both Edema and Apoptosis in Mice. *Sci. Rep.* **5,** 13807 (2015).

48. Page, E., Winterfield, J., Goings, G., Bastawrous, A. & Upshaw-Earley, J. Water channel proteins in rat cardiac myocyte caveolae: osmolarity-dependent reversible internalization. *Am. J. Physiol.* **274,** H1988-2000 (1998).

49. Kozera, L., White, E. & Calaghan, S. Caveolae act as membrane reserves which limit mechanosensitive I(Cl,swell) channel activation during swelling in the rat ventricular myocyte. *PloS One* **4,** e8312 (2009).

50. Rutkovskiy, A., Valen, G. & Vaage, J. Cardiac aquaporins. *Basic Res. Cardiol.* **108,** 393 (2013).

51. Nielsen, S. *et al.* Physiology and pathophysiology of renal aquaporins. *J. Am. Soc. Nephrol. JASN* **10,** 647–663 (1999).

52. Delporte, C., Bryla, A. & Perret, J. Aquaporins in Salivary Glands: From Basic Research to Clinical Applications. *Int. J. Mol. Sci.* **17,** (2016).

53. Yao, X., Derugin, N., Manley, G. T. & Verkman, A. S. Reduced brain edema and infarct volume in aquaporin-4 deficient mice after transient focal cerebral ischemia. *Neurosci. Lett.* **584,** 368–372 (2015).

54. Butler, T. L. *et al.* Cardiac aquaporin expression in humans, rats, and mice. *Am. J. Physiol. Heart Circ. Physiol.* **291,** H705-713 (2006).

55. Warth, A. *et al.* Upregulation of the water channel aquaporin-4 as a potential cause of postischemic cell swelling in a murine model of myocardial infarction. *Cardiology* **107,** 402–410 (2007).

56. Braunwald, E. & Kloner, R. A. Myocardial reperfusion: a double-edged sword? *J. Clin. Invest.* **76,** 1713–1719 (1985).

57. Kloner, R. A. Does reperfusion injury exist in humans? *J. Am. Coll. Cardiol.* **21,** 537–545 (1993).

58. Murry, C. E., Jennings, R. B. & Reimer, K. A. Preconditioning with ischemia: a delay of lethal cell injury in ischemic myocardium. *Circulation* **74,** 1124–1136 (1986).

59. Garcia-Dorado, D. & Piper, H. M. Postconditioning: reperfusion of 'reperfusion injury' after hibernation. *Cardiovasc. Res.* **69,** 1–3 (2006).

60. Cabrera-Fuentes, H. A. *et al.* Meeting report from the 2nd International Symposium on New Frontiers in Cardiovascular Research. Protecting the cardiovascular system from ischemia: between bench and bedside. *Basic Res. Cardiol.* **111,** 7 (2016).

61. Cung, T.-T. *et al.* Cyclosporine before PCI in Patients with Acute Myocardial Infarction. *N. Engl. J. Med.* **373,** 1021–1031 (2015).

62. Garcia-Dorado, D. *et al.* Intracoronary injection of adenosine before reperfusion in patients with. *Int. J. Cardiol.* **177,** 935–941 (2014).

63. Alburquerque-Bejar, J. J. *et al.* Combination therapy with remote ischaemic conditioning and insulin or exenatide enhances infarct size limitation in pigs. *Cardiovasc. Res.* **107,** 246–254 (2015).

64. Inserte, J. *et al.* Effect of acidic reperfusion on prolongation of intracellular acidosis and myocardial salvage. *Cardiovasc. Res.* **77,** 782–790 (2008).

65. Garcia-Dorado, D., Ruiz-Meana, M., Inserte, J., Rodriguez-Sinovas, A. & Piper, H. M. Calcium-mediated cell death during myocardial reperfusion. *Cardiovasc. Res.* **94,** 168–180 (2012).

66. Ruiz-Meana, M., Garcia-Dorado, D., Hofstaetter, B., Piper, H. M. & Soler-Soler, J. Propagation of cardiomyocyte hypercontracture by passage of Na(+) through gap junctions. *Circ. Res.* **85,** 280–287 (1999).

67. Ruiz-Meana, M. *et al.* Mitochondrial connexin43 as a new player in the pathophysiology of myocardial ischaemia-reperfusion injury. *Cardiovasc. Res.* **77,** 325–333 (2008).

68. Sanz, E. *et al.* Dissociation between anti-infarct effect and anti-edema effect of ischemic preconditioning. *Am. J. Physiol.* **268,** H233-241 (1995).

69. Inserte, J., Barba, I., Hernando, V. & Garcia-Dorado, D. Delayed recovery of intracellular acidosis during reperfusion prevents calpain activation and determines protection in postconditioned myocardium. *Cardiovasc. Res.* **81,** 116–122 (2009).

70. Chouchani, E. T. *et al.* Ischaemic accumulation of succinate controls reperfusion injury through mitochondrial ROS. *Nature* **515,** 431–435 (2014).

71. Kovacs, M., Toth, J., Hetenyi, C., Malnasi-Csizmadia, A. & Sellers, J. R. Mechanism of blebbistatin inhibition of myosin II. *J. Biol. Chem.* **279,** 35557–35563 (2004).

72. Inserte, J., Garcia-Dorado, D., Hernando, V. & Soler-Soler, J. Calpain-mediated impairment of Na+/K+-ATPase activity during early reperfusion contributes to cell death after myocardial ischemia. *Circ. Res.* **97,** 465–473 (2005).

73. Garcia-Dorado, D. & Oliveras, J. Myocardial oedema: a preventable cause of reperfusion injury? *Cardiovasc. Res.* **27,** 1555–1563 (1993).

74. Bekkers, S. C. A. M., Yazdani, S. K., Virmani, R. & Waltenberger, J. Microvascular obstruction: underlying pathophysiology and clinical diagnosis. *J. Am. Coll. Cardiol.* **55,** 1649–1660 (2010).

75. Tranum-Jensen, J. *et al.* Tissue osmolality, cell swelling, and reperfusion in acute regional myocardial ischemia in the isolated porcine heart. *Circ. Res.* **49,** 364–381 (1981).

76. Weis, S. *et al.* Src blockade stabilizes a Flk/cadherin complex, reducing edema and tissue injury following myocardial infarction. *J. Clin. Invest.* **113,** 885–894 (2004).

77. Schwarz, E. R. *et al.* Evaluation of the effects of intramyocardial injection of DNA expressing vascular endothelial growth factor (VEGF) in a myocardial infarction model in the rat--angiogenesis and angioma formation. *J. Am. Coll. Cardiol.* **35,** 1323–1330 (2000).

78. Oliveira, M. A. B. de *et al.* Modes of induced cardiac arrest: hyperkalemia and hypocalcemia--literature review. *Rev. Bras. Cir. Cardiovasc. Orgao Of. Soc. Bras. Cir. Cardiovasc.* **29,** 432–436 (2014).

79. Hearse, D. J., Stewart, D. A. & Braimbridge, M. V. Hypothermic arrest and potassium arrest: metabolic and myocardial protection during elective cardiac arrest. *Circ. Res.* **36,** 481–489 (1975).

80. Friedrich, M. G. *et al.* The salvaged area at risk in reperfused acute myocardial infarction as visualized by cardiovascular magnetic resonance. *J. Am. Coll. Cardiol.* **51,** 1581–1587 (2008).

81. Kim, H. W. *et al.* Relationship of T2-Weighted MRI Myocardial Hyperintensity and the Ischemic Area-At-Risk. *Circ. Res.* **117,** 254–265 (2015).

82. Saeed, M., Van, T. A., Krug, R., Hetts, S. W. & Wilson, M. W. Cardiac MR imaging: current status and future direction. *Cardiovasc. Diagn. Ther.* **5,** 290–310 (2015).

83. Fernandez-Jimenez, R. *et al.* Pathophysiology Underlying the Bimodal Edema Phenomenon After Myocardial Ischemia/Reperfusion. *J. Am. Coll. Cardiol.* **66,** 816–828 (2015).

84. Fernandez-Jimenez, R. *et al.* Myocardial edema after ischemia/reperfusion is not stable and follows a bimodal pattern: imaging and histological tissue characterization. *J. Am. Coll. Cardiol.* **65,** 315–323 (2015).

85. Kellman, P. & Hansen, M. S. T1-mapping in the heart: accuracy and precision. *J. Cardiovasc. Magn. Reson.* **16,** 2 (2014).

86. Flett, A. S., Hayward, M. P. & Ashworth, M. T. Equilibrium contrast cardiovascular magnetic resonance for the measurement of diffuse myocardial fibrosis: preliminary validation in humans. *Circulation* **122,** (2010).

87. Ugander, M., Bagi, P. S. & Oki, A. J. Myocardial edema as detected by pre-contrast T1 and T2 MRI delineates area at risk associated with acute myocardial infarction. *JACC Cardiovasc Imaging* **5,** (2012).

88. Dote, K., Sato, H., Tateishi, H., Uchida, T. & Ishihara, M. [Myocardial stunning due to simultaneous multivessel coronary spasms: a review of 5 cases]. *J. Cardiol.* **21,** 203–214 (1991).

89. Iga, K. *et al.* Transient segmental asynergy of the left ventricle of patients with various clinical manifestations possibly unrelated to the coronary artery disease. *Jpn. Circ. J.* **55,** 1061–1067 (1991).

90. Prasad, A., Lerman, A. & Rihal, C. S. Apical ballooning syndrome (Tako-Tsubo or stress cardiomyopathy): a mimic of acute myocardial infarction. *Am. Heart J.* **155,** 408–417 (2008).

91. Nunez-Gil, I. J. *et al.* Takotsubo cardiomyopathy and elderly adults: still a benign condition? *J. Am. Geriatr. Soc.* **63,** 404–407 (2015).

92. Wittstein, I. S. *et al.* Neurohumoral features of myocardial stunning due to sudden emotional stress. *N. Engl. J. Med.* **352,** 539–548 (2005).

93. Tsuchihashi, K. *et al.* Transient left ventricular apical ballooning without coronary artery stenosis: a novel heart syndrome mimicking acute myocardial infarction. Angina Pectoris-Myocardial Infarction Investigations in Japan. *J. Am. Coll. Cardiol.* **38,** 11–18 (2001).

94. Nunez Gil, I. J. *et al.* Characterization of Tako-tsubo Cardiomyopathy in Spain: Results from the RETAKO National Registry. *Rev. Espanola Cardiol. Engl. Ed* **68,** 505–512 (2015).

95. Sharkey, S. W. & Maron, B. J. Epidemiology and clinical profile of Takotsubo cardiomyopathy. *Circ. J. Off. J. Jpn. Circ. Soc.* **78,** 2119–2128 (2014).

96. Eitel, I. *et al.* Clinical characteristics and cardiovascular magnetic resonance findings in stress (takotsubo) cardiomyopathy. *JAMA* **306,** 277–286 (2011).

97. Abdel-Aty, H., Cocker, M. & Friedrich, M. G. Myocardial edema is a feature of Tako-Tsubo cardiomyopathy and is related to the severity of systolic dysfunction: insights from T2-weighted cardiovascular magnetic resonance. *Int. J. Cardiol.* **132,** 291–293 (2009).

98. Marathe, S. P. & Talwar, S. Surgery for transposition of great arteries: A historical perspective. *Ann. Pediatr. Cardiol.* **8,** 122–128 (2015).

99. MILLER, B. J. *et al.* The production and repair of interatrial septal defects under direct vision with the assistance of an extracorporeal pump-oxygenator circuit. *J. Thorac. Surg.* **26,** 598-616-632 (1953).

100. Zalaquett S, R. [Sixty years of mitral valve surgery]. *Rev. Med. Chil.* **137,** 1253–1260 (2009).

101. Barnard, C. N. The operation. A human cardiac transplant: an interim report of a successful operation performed at Groote Schuur Hospital, Cape Town. *South Afr. Med. J. Suid-Afr. Tydskr. Vir Geneeskd.* **41,** 1271–1274 (1967).

102. Barnard, C. N. What we have learned about heart transplants. *J. Thorac. Cardiovasc. Surg.* **56,** 457–468 (1968).

103. Diodato, M. & Chedrawy, E. G. Coronary artery bypass graft surgery: the past, present, and future of myocardial revascularisation. *Surg. Res. Pract.* **2014,** 726158 (2014).

104. Wiig, H. Pathophysiology of tissue fluid accumulation in inflammation. *J. Physiol.* **589,** 2945–2953 (2011).

105. Desai, K. V. *et al.* Mechanics of the left ventricular myocardial interstitium: effects of acute and chronic myocardial edema. *Am. J. Physiol. Heart Circ. Physiol.* **294,** H2428-2434 (2008).

106. Laine, G. A. & Allen, S. J. Left ventricular myocardial edema. Lymph flow, interstitial fibrosis, and cardiac function. *Circ. Res.* **68,** 1713–1721 (1991).

107. Laine, G. A. Microvascular changes in the heart during chronic arterial hypertension. *Circ. Res.* **62,** 953–960 (1988).

108. Davis, K. L., Mehlhorn, U., Laine, G. A. & Allen, S. J. Myocardial edema, left ventricular function, and pulmonary hypertension. *J. Appl. Physiol. Bethesda Md 1985* **78,** 132–137 (1995).

109. Brette, F. *et al.* Biphasic effects of hyposmotic challenge on excitation-contraction coupling in rat ventricular myocytes. *Am. J. Physiol. Heart Circ. Physiol.* **279,** H1963-1971 (2000).

110. Gonano, L. A. *et al.* Hypotonic swelling promotes nitric oxide release in cardiac ventricular myocytes: impact on swelling-induced negative inotropic effect. *Cardiovasc. Res.* **104,** 456–466 (2014).

111. Dongaonkar, R. M. *et al.* Award article: Microcirculatory Society Award for Excellence in Lymphatic Research: time course of myocardial interstitial edema resolution and associated left ventricular dysfunction. *Microcirc. N. Y. N 1994* **19,** 714–722 (2012).

112. Chavarria, L. *et al.* Brain magnetic resonance in experimental acute-on-chronic liver failure. *Liver Int. Off. J. Int. Assoc. Study Liver* **33,** 294–300 (2013).

113. Shigeno, T., Brock, M., Shigeno, S., Fritschka, E. & Cervos-Navarro, J. The determination of brain water content: microgravimetry versus drying-weighing method. *J. Neurosurg.* **57,** 99–107 (1982).

114. Marmarou, A., Poll, W., Shulman, K. & Bhagavan, H. A simple gravimetric technique for measurement of cerebral edema. *J. Neurosurg.* **49,** 530–537 (1978).

115. Bothe, H. W., Bodsch, W. & Hossmann, K. A. Relationship between specific gravity, water content, and serum protein extravasation in various types of vasogenic brain edema. *Acta Neuropathol. (Berl.)* **64,** 37–42 (1984).

116. Bhave, G. & Neilson, E. G. Body fluid dynamics: back to the future. *J. Am. Soc. Nephrol. JASN* **22,** 2166–2181 (2011).

117. HART, D. & METZ, J. The estimation of red cell volume with 51Cr-labelled erythrocytes and plasma volume with radioiodinated human serum albumin. *J. Clin. Pathol.* **15,** 459–461 (1962).

118. COTLOVE, E. Mechanism and extent of distribution of inulin and sucrose in chloride space of tissues. *Am. J. Physiol.* **176,** 396–410 (1954).

119. Bunger, R. Compartmented pyruvate in perfused working heart. *Am. J. Physiol.* **249,** H439-449 (1985).

120. Masuda, T., Dobson, G. P. & Veech, R. L. The Gibbs-Donnan near-equilibrium system of heart. *J. Biol. Chem.* **265,** 20321–20334 (1990).

121. Clarke, K., Anderson, R. E., Nedelec, J. F., Foster, D. O. & Ally, A. Intracellular and extracellular spaces and the direct quantification of molar intracellular concentrations of phosphorus metabolites in the isolated rat heart using 31P NMR spectroscopy and phosphonate markers. *Magn. Reson. Med.* **32,** 181–188 (1994).

122. Polimeni, P. I., Cutilletta, A. F. & Otten, M. D. Cation distributions in the hypertrophic myocardium (aortic constriction) of the rat. *Cardiovasc. Res.* **17,** 170–176 (1983).

123. Dobson, G. P. & Cieslar, J. H. Intracellular, interstitial and plasma spaces in the rat myocardium in vivo. *J. Mol. Cell. Cardiol.* **29,** 3357–3363 (1997).

124. Frank, J. S. & Langer, G. A. The myocardial interstitium: its structure and its role in ionic exchange. *J. Cell Biol.* **60,** 586–601 (1974).

125. Fisher, M. J. & Dillon, P. F. Phenylphosphonate: a 31P-NMR indicator of extracellular pH and volume in the isolated perfused rabbit bladder. *Circ. Res.* **60,** 472–477 (1987).

126. Cieslar, J., Huang, M. T. & Dobson, G. P. Tissue spaces in rat heart, liver, and skeletal muscle in vivo. *Am. J. Physiol.* **275,** R1530-1536 (1998).

127. Anzai, Y. *et al.* MR angiography with an ultrasmall superparamagnetic iron oxide blood pool agent. *J. Magn. Reson. Imaging JMRI* **7,** 209–214 (1997).

128. Misselwitz, B., Schmitt-Willich, H., Ebert, W., Frenzel, T. & Weinmann, H. J. Pharmacokinetics of Gadomer-17, a new dendritic magnetic resonance contrast agent. *Magma N. Y. N* **12,** 128–134 (2001).

129. Carr, D. H. *et al.* Gadolinium-DTPA as a contrast agent in MRI: initial clinical experience in 20 patients. *AJR Am. J. Roentgenol.* **143,** 215–224 (1984).

130. Jaspers, K. *et al.* MR angiography of collateral arteries in a hind limb ischemia model: comparison between blood pool agent Gadomer and small contrast agent Gd-DTPA. *PloS One* **6,** e16159 (2011).

131. Perea, R. J. *et al.* T1 mapping: characterisation of myocardial interstitial space. *Insights Imaging* **6,** 189–202 (2015).

132. Tanimoto, A., Mukai, M. & Kuribayashi, S. Evaluation of superparamagnetic iron oxide for MR imaging of liver injury: proton relaxation mechanisms and optimal MR imaging parameters. *Magn. Reson. Med. Sci. MRMS Off. J. Jpn. Soc. Magn. Reson. Med.* **5,** 89–98 (2006).

133. Lavin, B., Phinikaridou, A., Lorrio, S., Zaragoza, C. & Botnar, R. M. Monitoring vascular permeability and remodeling after endothelial injury in a murine model using a magnetic resonance albumin-binding contrast agent. *Circ. Cardiovasc. Imaging* **8,** (2015).

134. Gerber, B. L. *et al.* Myocardial first-pass perfusion cardiovascular magnetic resonance: history, theory, and current state of the art. *J. Cardiovasc. Magn. Reson. Off. J. Soc. Cardiovasc. Magn. Reson.* **10,** 18 (2008).

135. Koenig, S. H. Paramagnetic agents as tracers in magnetic resonance imaging. Extrapolations from Gd-DTPA to everything. *Acta Radiol. Suppl.* **374,** 17–23 (1990).

136. Anversa, P., Capasso, J. M., Puntillo, E., Sonnenblick, E. H. & Olivetti, G. Morphometric analysis of the infarcted heart. *Pathol. Res. Pract.* **185,** 544–550 (1989).

137. Wiener, J., Loud, A. V., Giacomelli, F. & Anversa, P. Morphometric analysis of hypertension-induced hypertrophy of rat thoracic aorta. *Am. J. Pathol.* **88,** 619–634 (1977).

138. Bell, R. M., Mocanu, M. M. & Yellon, D. M. Retrograde heart perfusion: the Langendorff technique of isolated heart perfusion. *J. Mol. Cell. Cardiol.* **50,** 940–950 (2011).

139. Aliev, M. K. *et al.* Water content and its intracellular distribution in intact and saline perfused rat hearts revisited. *Cardiovasc. Res.* **53,** 48–58 (2002).

140. Manning, W. J., Atkinson, D. J., Grossman, W., Paulin, S. & Edelman, R. R. First-pass nuclear magnetic resonance imaging studies using gadolinium-DTPA in patients with coronary artery disease. *J. Am. Coll. Cardiol.* **18,** 959–965 (1991).

141. Kim, H. W., Farzaneh-Far, A. & Kim, R. J. Cardiovascular Magnetic Resonance in Patients With Myocardial Infarction: Current and Emerging Applications. *J. Am. Coll. Cardiol.* **55,** 1–16 (2009).

142. COHEN, L., DJORDJEVICH, J. & ORMISTE, V. SERUM LACTIC DEHYDROGENASE ISOZYME PATTERNS IN CARDIOVASCULAR AND OTHER DISEASES, WITH PARTICULAR REFERENCE TO ACUTE MYOCARDIAL INFARCTION. *J. Lab. Clin. Med.* **64,** 355–374 (1964).

143. Ewen, L. M. & Griffiths, J. Patterns of enzyme activity following myocardial infarction and ischemia. *Am. J. Clin. Pathol.* **56,** 614–622 (1971).

144. Sahin, S., Karabey, Y., Kaynak, M. S. & Hincal, A. A. Potential use of freeze-drying technique for estimation of tissue water content. *Methods Find. Exp. Clin. Pharmacol.* **28,** 211–215 (2006).

145. Aliev, M. K., Khatkevich, A. N., Tsyplenkova, V. G., Meertsuk, F. E. & Kapelko, V. I. Tracer kinetics analysis of the extracellular spaces in saline perfused hearts. *Exp. Clin. Cardiol.* **6,** 188–194 (2001).

146. Eitel, I. *et al.* Prognostic significance and determinants of myocardial salvage assessed by cardiovascular magnetic resonance in acute reperfused myocardial infarction. *J. Am. Coll. Cardiol.* **55,** 2470–2479 (2010).

147. Wright, J., Adriaenssens, T., Dymarkowski, S., Desmet, W. & Bogaert, J. Quantification of myocardial area at risk with T2-weighted CMR: comparison with contrast-enhanced CMR and coronary angiography. *JACC Cardiovasc. Imaging* **2,** 825–831 (2009).

148. Aletras, A. H. *et al.* Retrospective determination of the area at risk for reperfused acute myocardial infarction with T2-weighted cardiac magnetic resonance imaging: histopathological and displacement encoding with stimulated echoes (DENSE) functional validations. *Circulation* **113,** 1865–1870 (2006).

149. Jennings, R. B., Schaper, J., Hill, M. L., Steenbergen, C. J. & Reimer, K. A. Effect of reperfusion late in the phase of reversible ischemic injury. Changes in cell volume, electrolytes, metabolites, and ultrastructure. *Circ. Res.* **56,** 262–278 (1985).

150. Goto, R., Tearle, H., Steward, D. J. & Ashmore, P. G. Myocardial oedema and ventricular function after cardioplegia with added mannitol. *Can. J. Anaesth. J. Can. Anesth.* **38,** 7–14 (1991).

151. Dunphy, G. *et al.* The effects of mannitol, albumin, and cardioplegia enhancers on 24-h rat heart preservation. *Am. J. Physiol.* **276,** H1591-1598 (1999).

152. Garcia-Dorado, D. *et al.* Favorable effects of hyperosmotic reperfusion on myocardial edema and infarct size. *Am. J. Physiol.* **262,** H17-22 (1992).

153. Ferreira, R. *et al.* Reduction of reperfusion injury with mannitol cardioplegia. *Ann. Thorac. Surg.* **48,** 77-83-84 (1989).

154. Montant, P., Sigovan, M., Revel, D. & Douek, P. MR imaging assessment of myocardial edema with T2 mapping. *Diagn. Interv. Imaging* **96,** 885–890 (2015).

155. Scholz, T. D., Martins, J. B. & Skorton, D. J. NMR relaxation times in acute myocardial infarction: relative influence of changes in tissue water and fat content. *Magn. Reson. Med.* **23,** 89–95 (1992).

156. Keir, S. L. & Wardlaw, J. M. Systematic review of diffusion and perfusion imaging in acute ischemic stroke. *Stroke J. Cereb. Circ.* **31,** 2723–2731 (2000).

157. Schilling, F. *et al.* MRI measurements of reporter-mediated increases in transmembrane water exchange enable detection of a gene reporter. *Nat. Biotechnol.* **35,** 75–80 (2017).

158. Fernandez-Jimenez, R. *et al.* Myocardial edema after ischemia/reperfusion is not stable and follows a bimodal pattern: imaging and histological tissue characterization. *J. Am. Coll. Cardiol.* **65,** 315–323 (2015).

159. Shim, J. K. *et al.* The effect of mannitol on oxygenation and creatine kinase MB release in patients undergoing multivessel off-pump coronary artery bypass surgery. *J. Thorac. Cardiovasc. Surg.* **133,** 704–709 (2007).

160. Buja, L. M. & Willerson, J. T. Abnormalities of volume regulation and membrane integrity in myocardial tissue slices after early ischemic injury in the dog: effects of mannitol, polyethylene glycol, and propranolol. *Am. J. Pathol.* **103,** 79–95 (1981).

161. Kellman, P., Wilson, J. R., Xue, H., Ugander, M. & Arai, A. E. Extracellular volume fraction mapping in the myocardium, part 1: evaluation of an automated method. *J Cardiovasc Magn Reson* **14,** (2012).

162. Kellman, P. *et al.* Extracellular volume fraction mapping in the myocardium, part 2: initial clinical experience. *J Cardiovasc Magn Reson* **14,** (2012).

163. Arheden, H., Saeed, M. & Higgins, C. B. Measurement of the distribution volume of gadopentetate dimeglumine at echo-planar mr imaging to quantify myocardial infarction: comparison with 99mtc-dtpa autoradiography in rats. *Radiology* **211,** (1999).

164. Kehr, E., Sono, M., Chugh, S. & Jerosch-Herold, M. Gadolinium-enhanced magnetic resonance imaging for detection and quantification of fibrosis in human myocardium in vitro. *Int J Cardiovasc Imaging* **24,** (2008).

165. Ferreira, V. M. *et al.* Non-contrast T1-mapping detects acute myocardial edema with high diagnostic accuracy: a comparison to T2-weighted cardiovascular magnetic resonance. *J Cardiovasc Magn Reson* **14,** (2012).

166. Dall'Armellina, E. *et al.* Cardiovascular magnetic resonance by non contrast T1-mapping allows assessment of severity of injury in acute myocardial infarction. *J. Cardiovasc. Magn. Reson. Off. J. Soc. Cardiovasc. Magn. Reson.* **14,** 15 (2012).

9 Annex: Articles publicats

9.1 Myocardial edema: a translational view. Garcia-Dorado D, Andres-Villarreal M, Ruiz-Meana M, Inserte J, Barba I. J Mol Cell Cardiol. 2012 May;52(5):931-9. Review.

9.2 Measuring Water Distribution in the Heart: Preventing Edema Reduces Ischemia-Reperfusion Injury. Andrés-Villarreal M, Barba I, Poncelas M, Inserte J, Rodriguez-Palomares J, Pineda V, Garcia-Dorado D. J Am Heart Assoc. 2016 Dec 17;5(12).

Journal of Molecular and Cellular Cardiology 52 (2012) 931–939

Contents lists available at SciVerse ScienceDirect

Journal of Molecular and Cellular Cardiology

journal homepage: www.elsevier.com/locate/yjmcc

Review article

Myocardial edema: A translational view

David Garcia-Dorado *, Mireia Andres-Villarreal, Marisol Ruiz-Meana, Javier Inserte, Ignasi Barba

Laboratory of Experimental Cardiology, Research Institute Cardiology Department Hospital Universitari Vall d'Hebron, Universitat Autònoma de Barcelona, Passeig de la Vall d'Hebron 119-129, 08035 Barcelona, Spain

ARTICLE INFO

Article history:
Received 7 November 2011
Received in revised form 9 January 2012
Accepted 10 January 2012
Available online 18 January 2012

Keywords:
Infarction
Ischemia–reperfusion
Aquaporins
Connexin hemichannles
Caveolae
Magnetic resonance imaging

ABSTRACT

Myocardial edema occurs in a large number of myocardial pathologies *particularly* during ischemia–reperfusion, and may contribute to cell dysfunction and death occurring in these conditions. Cardiomyocyte cell volume is tightly regulated by modifications in cytosolic osmolality. Changes in membrane water permeability through aquaporin and connexin hemichannels also contribute to cell volume changes while caveolae may be important in *sensing* cell volume changes sensing and associated signaling. Ischemia–reperfusion alters these mechanisms and increases microvascular permeability by endothelial hypercontracture-induced gap formation, endothelial cell death and basal membrane disruption. Detection of myocardial edema by MRI has many useful diagnostic applications in acute myocardial infarction and other conditions. However, discrimination between intra and extracellular myocardial edema is presently difficult at the bench and impossible at the bedside. Developing methods to differentiate intra from extracellular myocardial water should allow a better understanding of the mechanisms and consequences of myocardial edema and, as a consequence *lead to* new diagnostic and therapeutic applications.

Contents

Abbreviations: AQP, Aquaporins; CaM, Calmodulin; Cx, Connexins; DWI, Diffusion weighted Imaging; eNOS, endothelial nitric oxide synthase; IR, ischemia–reperfusion; MI, myocardial infarction; MMP, matrix metalloproteinases; mPTP, mitochondrial permeability transition pore; MRI, Magnetic Resonance Imaging; NCX, Na^+-Ca^+ exchanger; NHE, Na^+-H^+ exchanger; PKG, Protein Kinase G; ROS, radical oxygen species; RVD, regulatory volume decrease; RVI, regulatory volume increase; VEGF, Vascular Endothelial Growth Factor.

* Corresponding author at: Cardiology Department Hospital Universitari Vall d'Hebron, Passeig de la Vall d'Hebron 119-129, 08035 Barcelona, Spain. Tel.: +34 934894038; fax: +34 93 4894032.
E-mail address: dgdorado@vhebron.net (D. Garcia-Dorado).

0022-2828/$ – see front matter © 2012 Elsevier Ltd. All rights reserved.
doi:10.1016/j.yjmcc.2012.01.010

1. Introduction

Myocardial edema occurs in many pathological situations [1,2]. It has been suggested to contribute to myocardial injury and dysfunction, and it is an important diagnostic marker in magnetic resonance imaging (MRI). However, none of these aspects of myocardial edema has been completely characterized. The mechanisms of cellular and interstitial edema and their contributions to myocardial injury are a matter of discussion [3,4] and its diagnostic value is far from definitively established [5].

In this article, we review the available knowledge on the mechanisms involved in the genesis of myocardial edema, its consequences, its contribution to different heart diseases and the methods to measure cardiac water content and distribution.

2. Physiology of myocardial water balance

Tight water regulation is essential to maintain life in all cellular beings. As the complexity of organisms increases with evolution, water regulation becomes more sophisticated. In vertebrates, water control includes cell volume control, tissue fluid balance and whole body water homeostasis.

2.1. Control of cell volume in cardiomyocytes

2.1.1. Osmotic forces

Water movement across cell membranes is passive and determined by osmotic gradients and membrane permeability to water. However, ionic homeostasis is an expensive energy consuming process [6]. Cardiac cells maintain ionic gradients across their membranes that result in a membrane potential close to −80 mV during diastole, mainly due to the uneven distribution of K^+ [7]. During systolic depolarization Na^+ enters rapidly *into* the cell due to the large concentration and voltage gradients. Repolarization is mainly achieved through K^+ efflux. Intracellular Na^+ concentration is maintained by the action of the Na^+ pump (Na^+K^+ATPase). The electrochemical gradient of Na^+ generated by the Na^+K^+ATPase is coupled to and maintains other ionic gradients; in particular the Ca^{2+}gradients (by extruding the Ca^{2+}that enters the cell with each action potential) through Na^+-Ca^{2+} exchanger (NCX) [7]. Energy deficiency tends thus to result in Na^+ overload and cell swelling [8,9].

Na^+ movements are also essential for intracellular pH regulation. H^+ extrusion is largely *dependent* on Na^+ influx through Na^+-H^+ exchange (NHE) or Na^+-HCO_3^- co-transporter. Thus, rapid changes in pH induce changes in cell volume and vice versa [8]. Correction of intracellular acidosis is coupled to Na^+ influx and volume gain [10]. Under physiologic conditions, changes in cell volume tend to be small and transient due to the existence of finely tuned regulatory mechanisms [11] known as regulatory volume decrease (RVD) and regulatory volume increase (RVI) [11,12]. Both RVD and RVI are based on regulation of ion transport across cell membranes and control of organic osmolytes. In the case of cell swelling, cell extrudes small organic osmolytes and ions (mainly K^+ and Cl^-, through specific channels) and thus reduces cell volume [11]. On the other hand, cell shrinkage activates specific ion transporters which increase the organic osmolyte pool and tends to restore osmotic equilibrium across cell membrane. This is mainly accomplished through activation of Na^+-K^+-2Cl^--cotransporter thus up taking the three ions, as well as by the gain of Na^+ and Cl^- through the NHE and Cl^--HCO_3^- exchanger. Catabolization of glycogen and membrane phospholipids leads to a gain of organic osmolytes favoring water influx. Fig. 1 shows the mechanisms involved in cell volume control.

2.1.2. Channels

It is generally *considered* that water moves passively in and out the cell but the exact molecular mechanisms regulating the forces behind water movement are not completely elucidated. Recently, interest has risen on transmembrane channels that could play important roles in water homeostasis.

Aquaporins (AQP) are a big family of membrane proteins with six transmembrane helices which usually oligomerize into tetramers forming pores. Those pores are highly permeable to water and other uncharged small solutes and play an important role in water transport and osmoregulation. Their involvement in renal function and salivary production in mammals is well known [13]. AQP have also been found in human cardiomyocyte plasma membrane [14] but their function there is not well established. Sarcolemmal AQP-4 of cardiomyocytes is enhanced after ischemia; in addition, AQP-4 mRNA expression is higher in myocytes after ischemia and its upregulation has been associated with increased infarct size [15]. A reduction in the function of AQP-4 in *mouse* brain reduces edema and necrosis induced by ischemia [16].

Colocalization of AQP-1 and caveolin-3 has been described in rat cardiomyocytes and those complexes seem to be related to osmosensing and regulation of water permeability [17]. AQP-1 is present in microvascular and lymphatic endothelium and may contribute to water fluxes between vascular, interstitial and lymphatic spaces [18]. AQP-7, present in cardiac capillaries, may contribute to endothelial cell volume regulation [19] and extracellular edema formation. These data suggest that AQP may have a role in the ischemia–reperfusion (IR) injury through regulation of cardiomyocyte volume.

Connexins (Cx) are proteins with four transmembrane segments which form hemichannels through oligomerization of six Cx units. The connection between two hemichannels of adjacent cells forms the intercellular channel, involved in cell-to-cell communication in vertebrates. Gap junctions are specialized membrane regions containing clusters of such intercellular channels. Besides this well known function, there is evidence that Cx in the hemichannel conformation play a role in cell volume regulation [20]. Experiments performed on different cell types suggest that opening of Cx43 hemichannels leads to cell volume increase while this effect can be avoided by preventing the hemichannel opening [20]. A relationship between AQP4 and Cx43 in astrocytes has been described in mice [21]. The AQP4-knockdown leads to down regulation of Cx43 in mouse astrocytes, but at present, this link has not been demonstrated so far in human cells or in cardiomyocytes. Colocalization of Cx43 and caveolin-1 (the main structural protein of caveolae) has been demonstrated in mice endothelium; this link seems to be related with vascular tone through the endothelium-derived hyperpolarizing factor [22]. Cx43 is also expressed in endothelial cells, together with Cx37 and Cx40 [23], and may also contribute to cell volume regulation. In addition to Cx43, Cx40 and Cx45 are also expressed in minor quantities in cardiomyocytes, although their expression may be higher in specialized cardiomyocyte populations or under pathologic conditions [24].

Finally, pannexins, a recently discovered family of proteins with a high degree of structural similarity with Cxs but without significant

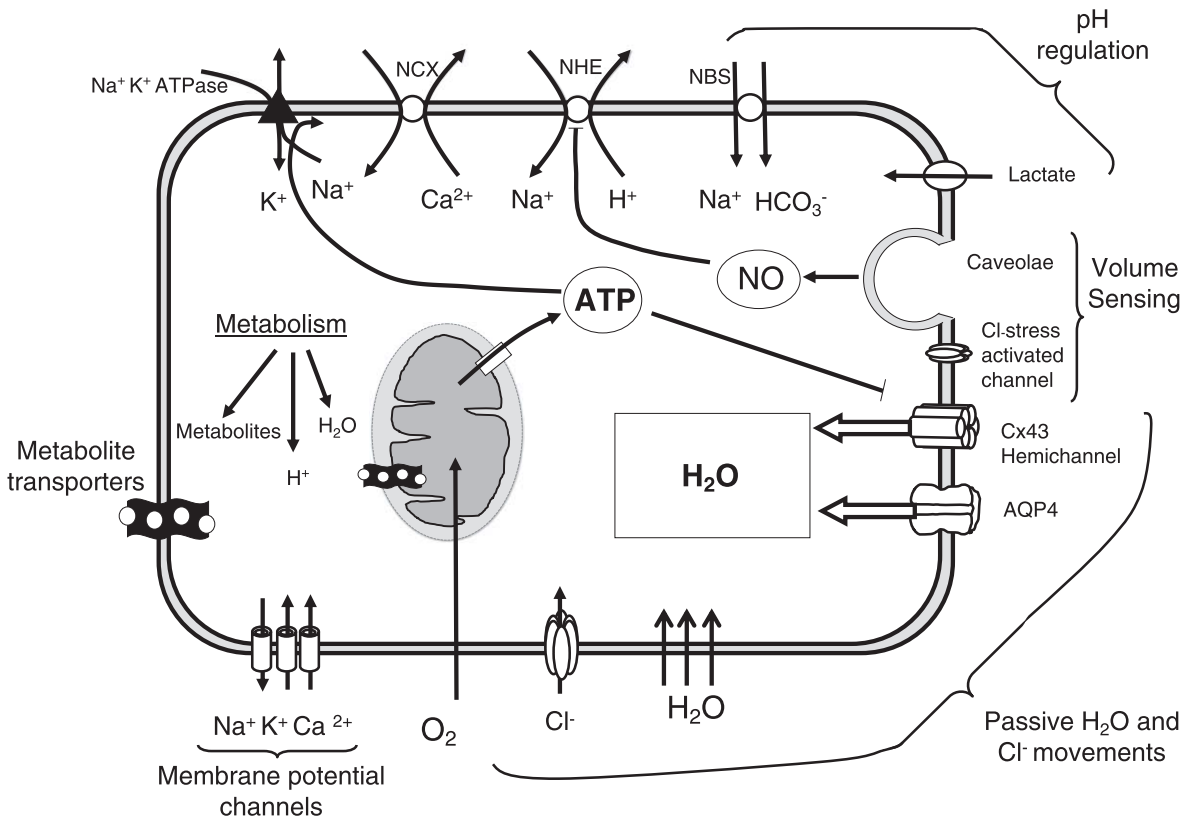

Fig. 1. Cell volume control cardiomyocytes.Control of cell volume in cardiomyocytes depends on mechanisms controlling intracellular osmotic pressure, including ion homeostasis and metabolism, and water transport through sarcolemmal channels and membrane diffusion. Regulation of intracellular pH is an important element in osmotic regulation. All these elements can be influenced by energy metabolism. Caveolae play a role in adaptation to changes in cell volume and stretch-induced signaling.

homology with these proteins, have been demonstrated in the heart [25]. Pannexins form transmembrane channels not coupled to opposing channels from adjacent cells and have been proposed to be involved in cell volume regulation [25].

2.1.3. Cell volume sensing

Cell volume sensing is achieved mainly through mechanical and chemical signals [26]. Mechanosensing is provided in part by specific mechanosensitive channels, which do open when the membrane stretches, thus allowing calcium influx into the cell [27]. There is evidence that cytoskeleton distortion may activate mechanosensitive channels and modify ion fluxes [28].

Sarcolemma plays also a key role in cell response to changes in cell volume. Caveolae are specialized regions of cell membrane forming invaginations and containing a large number and variety of signaling molecules [29], are present in most cell types including myocytes and endothelial cells, and are involved in many cellular processes related to tissue water control, including mechanosensing, ion channel regulation and endothelial permeability [30].

Caveolins are the main scaffolding proteins involved in caveolae formation, caveolin-1 is the ubiquitous isoform (expressed in endothelial cells) while the presence of caveolin-3 has been demonstrated in myocytes. Alterations in caveolae have been associated with atherosclerosis, hypertension, endothelial dysfunction, myocardial hypertrophy, remodeling and heart failure [31,32]. Caveolae structure and assembly can be affected by the presence of cell swelling [33]: caveolae may act as membrane reservoirs able to unfold in case of increased membrane stress due to cell swelling and thus prevent membrane rupture while losing caveolar structure [33]. This distortion of caveolae could explain some of the mechanisms triggered and signaling pathways affected by cell swelling. The interaction between eNOS (endothelial nitric oxide synthase), calmodulin (CaM) and caveolin seems particularly relevant [34]; eNOS activation by CaM needs eNOS dissociation from caveolin [35]. Very interestingly, recent studies have demonstrated that membrane stretching may cause flattening of caveola resulting in rapid caveolae disassembly [33] with important signaling effects. As NO plays a main role in cardiac function (both at microvascular and cardiomyocytes level) its modulation by caveolae changes is probably physiologically important. NO-dependent-PKG (Protein Kinase G) signaling has been shown to modulate cell volume by mechanisms including NHE inhibition [36].

2.1.4. Intracellular water distribution

A few layers of water molecules, called bound water or interfacial water, which provide hydration to the macromolecule, surround macromolecules. Bound water has different physical properties than free water, i.e. freezing temperature is lower and it *is distinct from* the aqueous media where solutes can diffuse freely. Bound water is thought to be 5% of total water and can be analyzed by magnetic resonance techniques based on spectroscopy [37]. When cell damage occurs, the disturbed proteins may release some bound water and therefore free water increases without a gain in the total cellular water content [38].

Myocardial water content is around 79 g per 100 g of fresh myocardial tissue (61.5 g intracellular water and 17.5 g extracellular water), with 34.6% of fresh tissue being water among myofibrils, 18% water in mitochondria and much smaller fractions in the remaining organelles [39]. Organelles, in particular mitochondria, have tight control mechanisms of volume and water content [40]. Regulation of mitochondrial volume is particularly important. In ventricular cardiac myocytes, mitochondria may occupy as much as 40% of total cellular volume, tightly packaged between myofibrils and underneath the

plasma membrane [41]. Mitochondria may tolerate an increase up to 30% of their volume without disruption of their integrity [42], which could affect total cell volume. Mitochondrial swelling is the result of osmotic water movement between cytosol and mitochondrial matrix and represents an important signaling transduction mechanism, with multiple (patho)physiological functions [40,43]. Changes in cytosolic osmolality affect mitochondrial volume. Increase or contraction of mitochondrial matrix volume have an impact on electron transport rate and ATP generation, radical oxygen species (ROS) production, apoptotic death and other cellular processes [44,45]. Due to their small size, mitochondria have a high surface to volume ratio, facilitating the achievement of a very rapid osmotic equilibrium in response to osmotic gradient [46]. Osmotic water movement is mainly dependent on K^+ fluxes, specifically mitochondrial K^+ influx through K^+ channels (either ATP-sensitive or calcium-activated), and K^+ extrusion via K^+/H^+ antiporter [47]. It has been postulated that the protective effect exerted by the opening of K^+ channels is due to the resulting matrix swelling that improves mitochondrial respiratory efficiency, which is particularly relevant under IR injury [48].

AQP8 isoform has been shown to localize in mitochondrial membranes in several tissues including the heart, where it contributes to reversible regulation of matrix volume [49] as well as to the diffusion of hydrogen peroxide across membranes [50] and mitochondrial ammonia transport [51]. Recently, Cx43 has also been identified at the inner membrane of subsarcolemmal mitochondria where it plays a role in water influx and K^+ permeability probably by forming hemichannel-like structures [52–54]. Mitochondria from Cx43-deficient mice show attenuated ADP-stimulated respiration and a reduced respiratory control ratio as compared with controls, and have impaired ROS production in response to diazoxide [55]. Whether these effects are related to altered water transport across Cx43 hemichannels is not known. Interestingly, in situ hearts and cardiomyocytes isolated from mice with reduced mitochondrial Cx43 content could not be cardioprotected by pharmacological preconditioning [55,56], a maneuver that has been associated with mitochondrial swelling. Finally, Opening of mitochondrial permeability transition pore (mPTP), a large non-specific pore of unresolved molecular structure [57] that allows passage of molecules up to 1500 Da, has been suggested to be functionally involved in water transport [46]. Under physiological conditions, basal flickering of mPTP represents a Ca^{2+} signaling mechanism [58,59] whereas permanent opening of mPTP results in disruption of mitochondrial electrochemical gradient [60].

2.2. Extracellular water

At the organ level, water balance depends on the equilibrium between net water filtration at capillaries and lymphatic drainage. Capillary filtration depends on intravascular and interstitial hydrostatic pressure (P_c and P_i respectively), oncotic pressure in both compartments (π_c and π_i), microvascular filtration coefficient, K_f, (which depends on the microvascular surface area and permeability to water) and Staverman's osmotic reflection coefficient, σ, (thus meaning the relative permeability to plasma proteins, ranging from 0 to 1, unit meaning complete reflection and zero maxim permeability). All those components are included in the modified Starling-Landis equation (Eq. (1)) [61,62]. Net capillary filtration is the overall result of different filtration rates at different capillary segments. Capillary filtration may be negative at distal capillaries and under pathologic conditions (capillary reabsorption, see below, [63].

$$J_v = K_f(P_c - P_i) - \sigma(\pi_c - \pi_i) \quad (1)$$

Lymphatic drainage is favored by the mechanic work of the heart (cardiac cycle) and depends on the central venous pressure (as lymph vessels drain into the central venous system). Lymphatics drain and return to blood circulation approximately 2.5 times the total plasma volume each day. Mehlhorn and cols have studied in depth the contribution of lymphatic drainage to heart fluid balance in normal and pathologic conditions as well during cardiac surgery [64,65]. Conditions increasing filtration through capillaries or decreasing lymphatic drainage would increase myocardial water content. Capillary filtration increases when capillary hydrostatic pressure rises (this occurs with systemic hypertension, reduction of myocardial venous return due to increase in coronary sinus [66], right chambers or central venous system pressure), when intravascular oncotic pressure decreases or interstitial oncotic pressure increases and also when microvasculature filtration coefficient rises (inflammatory response: vasodilatation, capillary recruitment, endothelial damage…) [1,67].

3. Myocardial edema secondary to ischemia–reperfusion

IR induces intra and extracellular myocardial edema that accompany not only myocardial infarction (MI), but also angina, apical ballooning [68,69], cardiopulmonary bypass with cardioplegia and heart transplantation or resuscitation [70].

3.1. Cardiomyocyte swelling

Myocardial ischemia creates an intra and extracellular increase of osmolality due to the accumulation of end-products of cellular anaerobic metabolism. Intracellular edema develops during ischemia at the expense of interstitial fluid due to the loss of transmembrane potential, Na^+Cl^- uptake and production of small molecules from anaerobic metabolism [71]. During ischemia cell swelling develops without an increase of total tissue water content because ischemic myocardial tissue is excluded from the circulation. Upon reperfusion, the rapid washout of extracellular osmotically active molecules generates a transsarcolemmal osmotic gradient that leads to water influx and cell swelling. In addition, it has been proposed that the loss of ionic homeostasis is a major cause for water influx in the reperfused cardiomyocyte [8,72,73]. During IR, dysfunctional Na^+K^+ATPase impairs normalization of intracellular Na^+ and Cl^- accumulated as consequence of the correction of intracellular acidosis produced by energy deprivation. Experiments with transporter inhibitors have demonstrated that pH_i recovery at reperfusion and the concomitant cell swelling are mainly mediated by NHE and $NaHCO_3^-$ cotransport [8]. Fig. 2 shows a diagram with main changes during IR leading to cell swelling.

3.2. Interstitial edema

Myocardial IR induces interstitial edema through several mechanisms. During ischemia, catabolites accumulate in ischemic cells and difuse to the interstitial space and osmolality increases in the intra and extra-cellular space. At the same time the stop of flow causes a drop in hidrostatic pressure in the intravascular space that favors fluid reabsorption at capillaries [63]. At the beginning of reperfusion the intravascular space is suddenly occupied by blood with physiologic osmolarity and tonicity as well as normal values of Na^+, Cl^-, proteins and the rest of ions and molecules usually present in blood. Then, an osmotic gradient between the intravascular and interstitial spaces develops and water moves from the vascular space to the interstitium, tending to restore the osmotic equilibrium, i.e. increased J_v due to enhanced $[\pi_i - \pi_c]$. In addition, endothelial damage caused by ischemia and reperfusion leads to increased vascular permeability due to endothelial hypercontracture and endothelial gap formation [74] as well as distortion of ionic and transcellular transport (ie. increased J_v due to K_f and σ rise). Endothelial damage increases not only water permeability but also protein leakage thus enhancing interstitial edema. Platelet activation and the subsequent release of tissue factor and platelet activated factor favors transcellular transport through endothelial cells. Finally, inflammation mediators activated

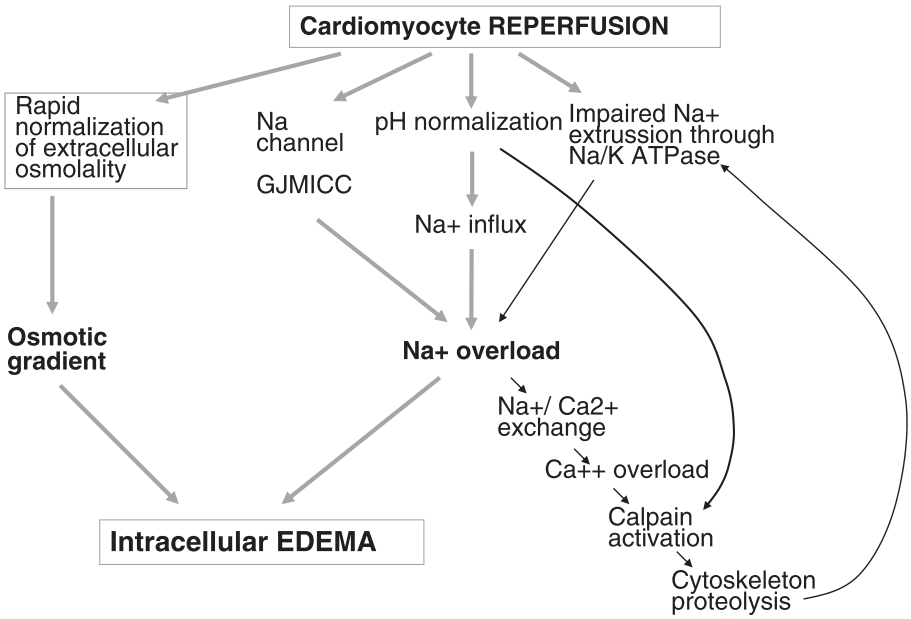

Fig. 2. Reperfusion-induced cardiomyocytes swelling.Rapid normalization of extracellular pH, correction of acidosis and Na^+ overload, favored by Ca^{2+} overload and energy deficiency are key determinants of reperfusion-induced cell swelling.

during and after IR, like Vascular Endothelial Growth Factor (VEGF), matrix metalloproteinases (MMP) and thrombin [75–77] contribute to endothelial necrosis, basal membrane proteolysis of endothelial cells and hemorrhage [78]. Reactive hyperemia after ischemia also enhances capillary filtration (J_v) towards the interstitium through an increase of P_c.

After MI, an increase in VEGF levels takes place and contributes to detrimental myocardial edema. But, also induces angiogenesis that could reduce remodeling and favor long-term heart recovery [79]. Interestingly, Feng and cols. demonstrated that increased endothelial permeability due to VEGF takes place through a signaling pathway involving eNOS and caveolin-1 [80]. Severe microvascular injury due to long prolonged ischemia and reperfusion is associated with disruption of microvascular morphology, with loss of endothelial cells and disruption of the basal membrane that may result in interstitial hemorrhage, no-reflow and intramyocardial hemorrhage phenomenon [78,81]. Fig. 3 shows a diagram with IR mechanisms involved in interstitial edema development.

3.3. Contribution of myocardial edema to ischemia–reperfusion injury

It has been proposed that myocardial edema induced by reperfusion may contribute to cell death. Stretch induced by swelling per se is not able to disrupt the sarcolemma [3,82]. However, stress caused by acute cell swelling during reperfusion cooperates with an increased sarcolemmal fragility and the development of hypercontracture to disrupt the sarcolemma [83]. Activation of phospholipases [84], the detergent effects of amphiphatic metabolites [85,85] and the proteolytic damage of the cytoskeletal scaffold [71] have been proposed to play a role. Hydrolysis of the structural protein α-fodrin by the activation during reperfusion of the Ca^{2+} dependent protease calpain is an important determinant of cell fragility [86]. Furthermore,

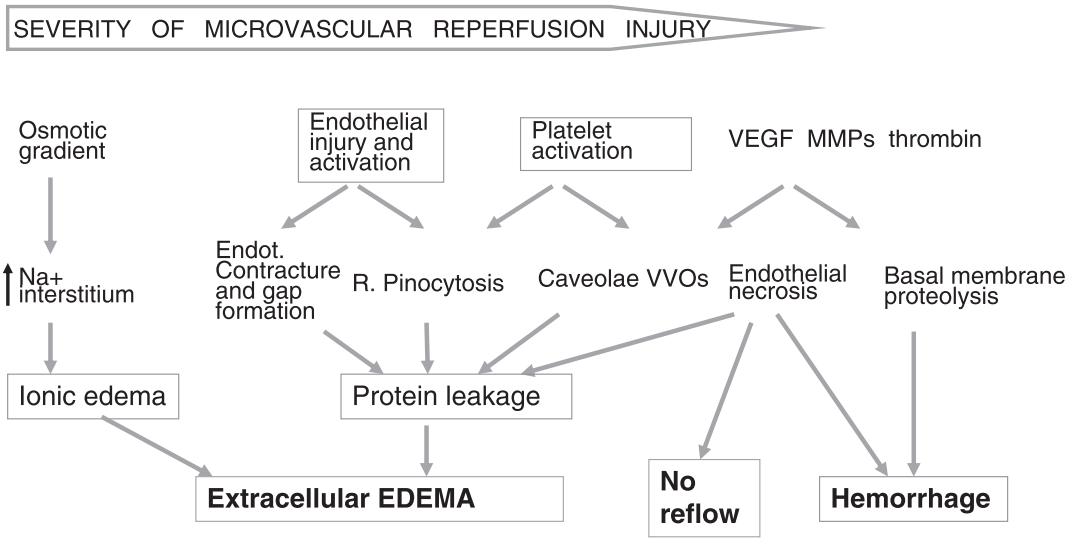

Fig. 3. Mechanisms of interstitial edema in reperfused myocardium.Osmotic interstitial edema occurs during reperfusion due to the abrupt normalization of intravascular osmolality. As the severity of ischemia–reperfusion injury increases, other mechanisms are added, from increased capilar permeability and protein leakage to severe microvascular disruption. See text for a detailed description.

the calpain mediated degradation of the ankyrin-fodrin complex, which serve as anchorage of Na^+K^+ATPase to the membrane-cytoskeleton, contributes to the impairment of Na^+K^+ATPase during early reperfusion and, therefore, favors cell swelling [87,88]. Mechanical stress caused by the hypercontraction of cardiomyocytes as consequence of the resupply of energy during the first minutes of reperfusion [89] in the presence of still elevated cytosolic Ca^{2+} concentration adds to that caused by osmotic swelling to produce sarcolemmal rupture. In addition to cell death, reperfusion-induced cardiomyocyte swelling has been proposed to contribute to myocardial stunning by increasing the distance between myofibrils actin and myosin [90]. In addition, NO produced as a consequence of caveolae flattening could contribute to reduced contractility through PKG signaling [91].

The results of pre-clinical studies show, in a quite concurrent way, that hypertonic reperfusion limits infarct size [67,92], but it has been suggested that the beneficial effects of some of the agents used to increase vascular osmotic pressure could be due in fact to their oxygen free radical-scavenging properties [93,94]. On the other hand, protective strategies at reducing infarct size, as ischemic preconditioning or postconditioning [95], limit myocardial edema [67]. Studies using intracoronary anoxic perfusion showed that both IPC and catabolite wash out before reperfusion, reduced the myocardial content of lactate at the end of ischemia, and the content of water after reperfusion in a similar amount, but catabolite washout alone did not reduce infarct size [4].

A key point in order to clarify the relation between the anti-edema and anti-infarct effects of cardioprotective interventions is to discriminate the contributions of intra and extracellular water to tissue edema. Alterations of vascular permeability caused by reperfusion-induced microvascular injury contribute to the non-reflow phenomenon [96] and more severe microvascular disruption may cause intramyocardial hemorrhage [78]. Although there is ample evidence that microvascular dysfunction (no-reflow, intramyocardial hemorrhage) is associated *with* poor prognosis in patients with acute MI undergoing reperfusion [97,98], the cause–effect relationship between both processes has not been fully clarified. Some studies suggest that severe microvascular dysfunction occurs only after cardiomyocyte death [99] and is thus a marker of large infarcts rather than a cause of them [78]. An important exception would be in any case, microvascular obstruction secondary to embolization from the culprit lesion during reperfusion, a mechanism completely different from endothelial-driven no-reflow. Its prevention by thromboaspiration appears to be beneficial at least under certain conditions [100].

Finally, reperfusion induced myocardial edema could also have some beneficial actions. Interstitial edema may increase wall thickness and stiffness immediately after reperfusion and may favor collagen deposition and fibrosis, and it has been proposed that this could attenuate infarct expansion and left ventricular remodeling independently of myocardial salvage [101].

3.4. Time course of myocardial edema in reperfused myocardium

Characterization of the time-course of reperfusion-induced myocardial edema and its determinants is of critical importance for the development of diagnostic and therapeutic applications. However, data on the dynamics of reperfusion-induced myocardial edema are very incomplete. We know from laboratory studies that edema appears during the initial few minutes of reperfusion [8,67,102,103] while studies with MRI (see below) in pig model have demonstrated that edema remains 40 days after MI [104]; studies in humans show that myocardial edema is not present 6 months after reperfusion [105] or just 100 days after the onset of stress cardiomyopathy [106]. However, the exact time course of edema and the factors that modulate it are not known. In particular the influence of the duration and severity of ischemia has not been characterized. Moreover, there is virtually a complete lack of information regarding the dynamics of cellular and interstitial edema. Since most cell death occurs early during reperfusion and energetic recovery is relatively rapid in surviving cardiomyocytes, it is expected that most myocardial edema observed days or weeks after reperfusion is extracellular, i.e. outside surviving cells.

3.5. Myocardial edema during cardiac surgery

During cardioplegic arrest, myocardium is exposed to ischemia and reperfusion, but their impact on myocardial edema is modified by the composition of the cardioplegic solution and by temperature, because hypothermia may affect cell metabolism and the activity of ion channels [107]. Cardioplegic solutions are hypooncotic and thus favor myocardial edema. In addition, cardiac arrest reduces lymphatic drainage, also contributing to myocardial edema. Finally, extracorporeal circulation induces an inflammatory response with white blood cell activation and high levels of circulating cytokines that increase capillary permeability and increase interstitial edema. Preservation of the explanted heart for transplantation is an extreme case of prolonged cardioplegic arrest. In this context hyperosmolar solutions used to perfuse the explanted hearts (like University of Wisconsin solution) have been developed, demonstrating a good protective profile [108] and are actually commonly used worldwide [109].

4. Myocardial edema in conditions other than ischemia–reperfusion

Increased afterload and inflammation may cause interstitial myocardial edema. Studies in a pulmonary artery banding animal model causing an increase in coronary sinus pressure, have shown the appearance of interstitial myocardial edema and the development of fibrosis [64,110]. Interestingly, the type of collagen that is synthesized appears to depend on the duration of myocardial edema. Acute edema increases collagen type I, while in chronic interstitial myocardial edema models, type I collagen fibers are replaced by type III and ventricular compliance is increased [111]. Increased afterload of the left ventricle has also been associated *with* increased myocardial microvascular permeability to macromolecules 4–6 weeks after inducing renovascular arterial hypertension [112].

Increased vascular permeability secondary to inflammation is the main mechanism of myocardial edema due to viral myocarditis, graft rejection and autoimmune or systemic diseases. Its detection with magnetic resonance imaging (MRI) allows the early diagnosis of these situations [113,114].

5. Measuringmyocardial edema

5.1. Myocardial edema in the laboratory

Total myocardial water content can be measured by tissue desiccation (at 85–110 °C), freeze-dry [115] or microgravity methods [116]. Water content in isolated cardiomyocytes can be measured by spectrometry-based light-scattering [117,118], morphometry [119], calcein equilibration [118] or gravity assays [120].

Differentiation of intra from extracellular water remains a largely unmet challenge. Some authors have used histology to estimate the interstitial edema and cell swelling [81,121,122] but sample processing can modify the structure and the process of *paraffin embedding* requires eliminating water from the sample. Another approach to determine water distribution is to use membrane-impermeable tracers; the intracellular space being determined as the difference between total and extracellular water. The most common EC markers are labeled high molecular weight polysaccharides like [^{14}C]hydroxymethyl inulin (first used by Grochowski and cols [123]) and [^{14}C] mannitol. However, this approach is not reliable in the presence of cell death due to the loss of plasma membrane integrity. In addition,

EC markers like inulin and low molecular weight markers (like $^{35}SO_4$ or ^{14}C-sucrose), reach in variable proportions the intracellular space in 18% and 28% respectively [121].

5.2. Measurement of myocardial edema with MRI

T2 weighted magnetic resonance imaging (T2W MRI) allows *estimation of* differences in the total water content in vivo [124] and this is the only way to determine in vivo and non-invasively the presence of edema. Despite being a powerful tool to identify myocardial edema, there are not MRI applications to differentiate water distribution in the heart. Diffusion weighted Imaging (DWI) measures how far water molecules move through a magnetic field in a given time. DWI methods have been used in parallel to T2W to study edema and also intra-extracellular water distribution in the brain [125]. However, these sequences have not been implemented yet in cardiac magnetic resonance imaging. Only preliminary reports of DWI data are available [126].

Although current MRI techniques provide only semi quantitative information on myocardial water content and do not permit reliable discrimination between intra and extracellular edema, they constitute a powerful and widely used tool to study myocardial edema in patients with many pathological conditions [127]. T2 cardiac MRI sequences have been suggested as an important method to non-invasively assess myocardial area at risk (AAR) both in animals and human studies [103,128,129]. Short-tau inversion recovery T2 sequences (T2-STIR) have been the most widely used for the detection and assessment of myocardial edema [128], but they have to be acquired before gadolinium administration [130]. Fat suppression and black blood sequences *can be used* to highlight edema and the contrast between the blood and myocardium respectively [131]. By using these techniques, cardiac MRI *enables the diagnosis of* myocardial ischemia, MI and its complications (non-reflow, hemorrhagic infarction, etc.), myocarditis and graft rejection with high specificity and sensitivity based on detection of myocardial edema.

6. Conclusion

Myocardial edema is a key element of myocardial pathophysiology that can be detected by MRI, which leads to many diagnostic applications. The mechanisms of myocardial edema induced by IR and other conditions are only partially understood, due in part to the lack of methods able to differentiate intra from extracellular water in vivo. Developing reliable, clinically usable methods able to discriminate intra form extracellular water should improve our understanding on the mechanisms and consequences of myocardial edema and allow the implementation of new diagnostic and therapeutic applications in many heart diseases, particularly in those involving myocardial ischemia and reperfusion. Characterization of the time course of myocardial edema in reperfused myocardium will be a big step forward in the development of these applications. Moreover, quantification of intracellular and interstitial myocardial edema by non-invasive methods could help to distinguish cell death occurring during ischemia from that having occurred upon reperfusion, and provide useful additional information in infarct size clinical trials evaluating cardioprotective interventions.

Disclosures

None.

Acknowledgments

This work was supported by the Spanish Ministries of Science (CICYT SAF/2008-03067), Redes temáticas de investigación cooperativa sanitaria-Red investigación enfermedades cardiovasculares (RETICS-RECAVA, RD06/0014/0025) and Fondo Investigación Sanitaria (FIS-PI080238 and FIS-PS09/02034). Mireia Andres-Villarreal is supported by a PROMISE grant. Ignasi Barba is a recipient of a Ramón y Cajal Fellowship.

References

[1] Garcia-Dorado D, Oliveras J. Myocardial oedema: a preventable cause of reperfusion injury? Cardiovasc Res 1993;27(9):1555–63.
[2] Mehlhorn U, Davis KL, Laine GA, Geissler HJ, Allen SJ. Myocardial fluid balance in acute hypertension. Microcirculation 1996;3(4):371–8.
[3] Butler TL, Egan JR, Graf FG, Au CG, McMahon AC, North KN, et al. Dysfunction induced by ischemia versus edema: does edema matter? J Thorac Cardiovasc Surg 2009;138(1):141–7 147.
[4] Sanz E, Garcia DD, Oliveras J, Barrabes JA, Gonzalez MA, Ruiz-Meana M, et al. Dissociation between anti-infarct effect and anti-edema effect of ischemic preconditioning. Am J Physiol 1995;268(1 Pt 2):H233–41.
[5] Hombach V, Merkle N, Bernhard P, Rasche V, Rottbauer W. Prognostic significance of cardiac magnetic resonance imaging: update 2010. Cardiol J 2010;17(6):549–57.
[6] Leaf A. Maintenance of concentration gradients and regulation of cell volume. Ann N Y Acad Sci 1959;72(12):396–404.
[7] Baumgarten CM, Fozzard HA. Cardiac resting and pacemaker potentials. In: Fozzard HA, Haber E, Jennings RB, Katz AM, Morgan HE, editors. The heart and cardiovascular system. Second ed. New York: Raven Press, Ltd; 1992. p. 963–1001.
[8] Inserte J, Garcia-Dorado D, Ruiz-Meana M, Solares J, Soler J. The role of Na+−H+ exchange occurring during hypoxia in the genesis of reoxygenation-induced myocardial oedema. J Mol Cell Cardiol 1997;29(4):1167–75.
[9] Vandenberg JI, Rees SA, Wright AR, Powell T. Cell swelling and ion transport pathways in cardiac myocytes. Cardiovasc Res 1996;32(1):85–97.
[10] Klein HH, Pich S, Bohle RM, Wollenweber J, Nebendahl K. Myocardial protection by Na(+)-H+ exchange inhibition in ischemic, reperfused porcine hearts. Circulation 1995;92(4):912–7.
[11] Hoffmann EK, Lambert IH, Pedersen SF. Physiology of cell volume regulation in vertebrates. Physiol Rev 2009;89(1):193–277.
[12] Lang F, Busch GL, Ritter M, Volkl H, Waldegger S, Gulbins E, et al. Functional significance of cell volume regulatory mechanisms. Physiol Rev 1998;78(1):247–306.
[13] Kruse E, Uehlein N, Kaldenhoff R. The aquaporins. Genome Biol 2006;7(2):206.
[14] Butler TL, Au CG, Yang B, Egan JR, Tan YM, Hardeman EC, et al. Cardiac aquaporin expression in humans, rats, and mice. Am J Physiol Heart Circ Physiol 2006;291(2):H705–13.
[15] Warth A, Eckle T, Kohler D, Faigle M, Zug S, Klingel K, et al. Upregulation of the water channel aquaporin-4 as a potential cause of postischemic cell swelling in a murine model of myocardial infarction. Cardiology 2007;107(4):402–10.
[16] Manley GT, Fujimura M, Ma T, Noshita N, Filiz F, Bollen AW, et al. Aquaporin-4 deletion in mice reduces brain edema after acute water intoxication and ischemic stroke. Nat Med 2000;6(2):159–63.
[17] Page E, Winterfield J, Goings G, Bastawrous A, Upshaw-Earley J. Water channel proteins in rat cardiac myocyte caveolae: osmolarity-dependent reversible internalization. Am J Physiol 1998;274(6 Pt 2):H1988–2000.
[18] Gannon BJ, Carati CJ. Endothelial distribution of the membrane water channel molecule aquaporin-1: implications for tissue and lymph fluid physiology? Lymphat Res Biol 2003;1(1):55–66.
[19] Skowronski MT, Lebeck J, Rojek A, Praetorius J, Fuchtbauer EM, Frokiaer J, et al. AQP7 is localized in capillaries of adipose tissue, cardiac and striated muscle: implications in glycerol metabolism. Am J Physiol Renal Physiol 2007;292(3):F956–65.
[20] Quist AP, Rhee SK, Lin H, Lal R. Physiological role of gap-junctional hemichannels. Extracellular calcium-dependent isosmotic volume regulation. J Cell Biol 2000;148(5):1063–74.
[21] Nicchia GP, Srinivas M, Li W, Brosnan CF, Frigeri A, Spray DC. New possible roles for aquaporin-4 in astrocytes: cell cytoskeleton and functional relationship with connexin43. FASEB J 2005;19(12):1674–6.
[22] Saliez J, Bouzin C, Rath G, Ghisdal P, Desjardins F, Rezzani R, et al. Role of caveolar compartmentation in endothelium-derived hyperpolarizing factor-mediated relaxation: Ca2+ signals and gap junction function are regulated by caveolin in endothelial cells. Circulation 2008;117(8):1065–74.
[23] Brisset AC, Isakson BE, Kwak BR. Connexins in vascular physiology and pathology. Antioxid Redox Signal 2009;11(2):267–82.
[24] Severs NJ, Dupont E, Thomas N, Kaba R, Rothery S, Jain R, et al. Alterations in cardiac connexin expression in cardiomyopathies. Adv Cardiol 2006;42:228–42.
[25] Rodriguez-Sinovas A, Sanchez JA, Fernandez-Sanz C, Ruiz-Meana M, Garcia-Dorado D. Connexin and pannexin as modulators of myocardial injury. Biochim Biophys Acta in press. doi: 10.1016/j.bbamem.2011.07.041 [Electronic publication ahead of print].
[26] Wright AR, Rees SA. Cardiac cell volume: crystal clear or murky waters? A comparison with other cell types. Pharmacol Ther 1998;80(1):89–121.
[27] Haswell ES, Phillips R, Rees DC. Mechanosensitive channels: what can they do and how do they do it? Structure 2011;19(10):1356–69.
[28] Hayakawa K, Tatsumi H, Sokabe M. Actin stress fibers transmit and focus force to activate mechanosensitive channels. J Cell Sci 2008;121(Pt 4):496–503.
[29] PROGRAM. Proceedings of the Electron Microscope Society of America. J Appl Phys 1953;24:1414–25.
[30] Frank PG, Woodman SE, Park DS, Lisanti MP. Caveolin, caveolae, and endothelial cell function. Arterioscler Thromb Vasc Biol 2003;23(7):1161–8.

[31] Das M, Das DK. Caveolae, caveolin, and cavins: Potential targets for the treatment of cardiac disease. Ann Med in press doi:10.3109/07853890.2011.577445 [Electronic publication ahead of print].
[32] Fernandez-Hernando C, Yu J, Suarez Y, Rahner C, Davalos A, Lasuncion MA, et al. Genetic evidence supporting a critical role of endothelial caveolin-1 during the progression of atherosclerosis. Cell Metab 2009;10(1):48–54.
[33] Sinha B, Koster D, Ruez R, Gonnord P, Bastiani M, Abankwa D, et al. Cells respond to mechanical stress by rapid disassembly of caveolae. Cell 2011;144(3):402–13.
[34] Feron O, Dessy C, Moniotte S, Desager JP, Balligand JL. Hypercholesterolemia decreases nitric oxide production by promoting the interaction of caveolin and endothelial nitric oxide synthase. J Clin Invest 1999;103(6):897–905.
[35] Feron O, Belhassen L, Kobzik L, Smith TW, Kelly RA, Michel T. Endothelial nitric oxide synthase targeting to caveolae. Specific interactions with caveolin isoforms in cardiac myocytes and endothelial cells. J Biol Chem 1996;271(37):22810–4.
[36] Inserte J, Barba I, Poncelas-Nozal M, Hernando V, Agullo L, Ruiz-Meana M, et al. cGMP/PKG pathway mediates myocardial postconditioning protection in rat hearts by delaying normalization of intracellular acidosis during reperfusion. J Mol Cell Cardiol 2011;50(5):903–9.
[37] Tompa K, Banki P, Bokor M, Kamasa P, Lasanda G, Tompa P. Interfacial water at protein surfaces: wide-line NMR and DSC characterization of hydration in ubiquitin solutions. Biophys J 2009;96(7):2789–98.
[38] Kuntz Jr ID, Brassfield TS, Law GD, Purcell GV. Hydration of macromolecules. Science 1969;163(3873):1329–31.
[39] Aliev MK, Dos SP, Hoerter JA, Soboll S, Tikhonov AN, Saks VA. Water content and its intracellular distribution in intact and saline perfused rat hearts revisited. Cardiovasc Res 2002;53(1):48–58.
[40] Kaasik A, Safiulina D, Zharkovsky A, Veksler V. Regulation of mitochondrial matrix volume. Am J Physiol Cell Physiol 2007;292(1):C157–63.
[41] Palmer JW, Tandler B, Hoppel CL. Biochemical properties of subsarcolemmal and interfibrillar mitochondria isolated from rat cardiac muscle. J Biol Chem 1977;252(23):8731–9.
[42] Das M, Parker JE, Halestrap AP. Matrix volume measurements challenge the existence of diazoxide/glibencamide-sensitive KATP channels in rat mitochondria. J Physiol 2003;547(Pt 3):893–902.
[43] Lee WK, Thevenod F. A role for mitochondrial aquaporins in cellular life-and-death decisions? Am J Physiol Cell Physiol 2006;291(2):C195–202.
[44] Gogvadze V, Robertson JD, Enoksson M, Zhivotovsky B, Orrenius S. Mitochondrial cytochrome c release may occur by volume-dependent mechanisms not involving permeability transition. Biochem J 2004;378(Pt 1):213–7.
[45] Halestrap AP. The regulation of the oxidation of fatty acids and other substrates in rat heart mitochondria by changes in the matrix volume induced by osmotic strength, valinomycin and Ca2+. Biochem J 1987;244(1):159–64.
[46] Gena P, Fanelli E, Brenner C, Svelto M, Calamita G. News and views on mitochondrial water transport. Front Biosci 2009;14:4189–98.
[47] Garlid KD, Paucek P. Mitochondrial potassium transport: the K(+) cycle. Biochim Biophys Acta 2003;1606(1–3):23–41.
[48] Garlid KD, Dos SP, Xie ZJ, Costa AD, Paucek P. Mitochondrial potassium transport: the role of the mitochondrial ATP-sensitive K(+) channel in cardiac function and cardioprotection. Biochim Biophys Acta 2003;1606(1–3):1–21.
[49] Calamita G, Ferri D, Gena P, Liquori GE, Cavalier A, Thomas D, et al. The inner mitochondrial membrane has aquaporin-8 water channels and is highly permeable to water. J Biol Chem 2005;280(17):17149–53.
[50] Bienert GP, Moller AL, Kristiansen KA, Schulz A, Moller IM, Schjoerring JK, et al. Specific aquaporins facilitate the diffusion of hydrogen peroxide across membranes. J Biol Chem 2007;282(2):1183–92.
[51] Soria LR, Fanelli E, Altamura N, Svelto M, Marinelli RA, Calamita G. Aquaporin-8-facilitated mitochondrial ammonia transport. Biochem Biophys Res Commun 2010;393(2):217–21.
[52] Boengler K, Stahlhofen S, van de SA, Gres P, Ruiz-Meana M, Garcia-Dorado D, et al. Presence of connexin 43 in subsarcolemmal, but not in interfibrillar cardiomyocyte mitochondria. Basic Res Cardiol 2009;104(2):141–7.
[53] Miro-Casas E, Ruiz-Meana M, Agullo E, Stahlhofen S, Rodriguez-Sinovas A, Cabestrero A, et al. Connexin43 in cardiomyocyte mitochondria contributes to mitochondrial potassium uptake. Cardiovasc Res 2009;83(4):747–56.
[54] Ruiz-Meana M, Rodriguez-Sinovas A, Cabestrero A, Boengler K, Heusch G, Garcia-Dorado D. Mitochondrial connexin43 as a new player in the pathophysiology of myocardial ischaemia–reperfusion injury. Cardiovasc Res 2008;77(2):325–33.
[55] Heinzel FR, Luo Y, Li X, Boengler K, Buechert A, Garcia-Dorado D, et al. Impairment of diazoxide-induced formation of reactive oxygen species and loss of cardioprotection in connexin 43 deficient mice. Circ Res 2005;97(6):583–6.
[56] Rodriguez-Sinovas A, Boengler K, Cabestrero A, Gres P, Morente M, Ruiz-Meana M, et al. Translocation of connexin 43 to the inner mitochondrial membrane of cardiomyocytes through the heat shock protein 90-dependent TOM pathway and its importance for cardioprotection. Circ Res 2006;99(1):93–101.
[57] He L, Lemasters JJ. Regulated and unregulated mitochondrial permeability transition pores: a new paradigm of pore structure and function? FEBS Lett 2002;512(1–3):1–7.
[58] Elrod JW, Wong R, Mishra S, Vagnozzi RJ, Sakthievel B, Goonasekera SA, et al. Cyclophilin D controls mitochondrial pore-dependent Ca(2+) exchange, metabolic flexibility, and propensity for heart failure in mice. J Clin Invest 2010;120(10):3680–7.
[59] Ichas F, Jouaville LS, Mazat JP. Mitochondria are excitable organelles capable of generating and conveying electrical and calcium signals. Cell 1997;89(7):1145–53.
[60] Baines CP. The mitochondrial permeability transition pore and ischemia–reperfusion injury. Basic Res Cardiol 2009;104(2):181–8.
[61] Dongaonkar RM, Stewart RH, Geissler HJ, Laine GA. Myocardial microvascular permeability, interstitial oedema, and compromised cardiac function. Cardiovasc Res 2010;87(2):331–9.
[62] Simard JM, Kent TA, Chen M, Tarasov KV, Gerzanich V. Brain oedema in focal ischaemia: molecular pathophysiology and theoretical implications. Lancet Neurol 2007;6(3):258–68.
[63] Kurbel S, Kurbel B, Belovari T, Maric S, Steiner R, Bozic D. Model of interstitial pressure as a result of cyclical changes in the capillary wall fluid transport. Med Hypotheses 2001;57(2):161–6.
[64] Laine GA, Allen SJ. Left ventricular myocardial edema. Lymph flow, interstitial fibrosis, and cardiac function. Circ Res 1991;68(6):1713–21.
[65] Mehlhorn U, Geissler HJ, Laine GA, Allen SJ. Myocardial fluid balance. Eur J Cardiothorac Surg 2001;20(6):1220–30.
[66] Pratt JW, Schertel ER, Schaefer SL, Esham KE, McClure DE, Heck CF, et al. Acute transient coronary sinus hypertension impairs left ventricular function and induces myocardial edema. Am J Physiol 1996;271(3 Pt 2):H834–41.
[67] Garcia-Dorado D, Theroux P, Munoz R, Alonso J, Elizaga J, Fernandez-Aviles F, et al. Favorable effects of hyperosmotic reperfusion on myocardial edema and infarct size. Am J Physiol 1992;262(1 Pt 2):H17–22.
[68] Abdel-Aty H, Cocker M, Meek C, Tyberg JV, Friedrich MG. Edema as a very early marker for acute myocardial ischemia: a cardiovascular magnetic resonance study. J Am Coll Cardiol 2009;53(14):1194–201.
[69] Nef HM, Mollmann H, Kostin S, Troidl C, Voss S, Weber M, et al. Tako-Tsubo cardiomyopathy: intraindividual structural analysis in the acute phase and after functional recovery. Eur Heart J 2007;28(20):2456–64.
[70] Sasaguri S, Sunamori M, Saito K, Suzuki A. Early change of myocardial water during acute cardiac allograft rejection. Jpn Circ J 1986;50(11):1113–9.
[71] Steenbergen C, Hill ML, Jennings RB. Volume regulation and plasma membrane injury in aerobic, anaerobic, and ischemic myocardium in vitro. Effects of osmotic cell swelling on plasma membrane integrity. Circ Res 1985;57(6):864–75.
[72] Anderson SE, Murphy E, Steenbergen C, London RE, Cala PM. Na-H exchange in myocardium: effects of hypoxia and acidification on Na and Ca. Am J Physiol 1990;259(6 Pt 1):C940–8.
[73] Tomita M, Gotoh F. Cascade of cell swelling: thermodynamic potential discharge of brain cells after membrane injury. Am J Physiol 1992;262(2 Pt 2):H603–10.
[74] Kasseckert SA, Schafer C, Kluger A, Gligorievski D, Tillmann J, Schluter KD, et al. Stimulation of cGMP signalling protects coronary endothelium against reperfusion-induced intercellular gap formation. Cardiovasc Res 2009;83(2):381–7.
[75] Gunduz D, Hirche F, Hartel FV, Rodewald CW, Schafer M, Pfitzer G, et al. ATP antagonism of thrombin-induced endothelial barrier permeability. Cardiovasc Res 2003;59(2):470–8.
[76] Mirabet M, Garcia-Dorado D, Inserte J, Barrabes JA, Lidon RM, Soriano B, et al. Platelets activated by transient coronary occlusion exacerbate ischemia–reperfusion injury in rat hearts. Am J Physiol Heart Circ Physiol 2002;283(3):H1134–41.
[77] Mirabet M, Garcia-Dorado D, Ruiz-Meana M, Barrabes JA, Soler-Soler J. Thrombin increases cardiomyocyte acute cell death after ischemia and reperfusion. J Mol Cell Cardiol 2005;39(2):277–83.
[78] Garcia-Dorado D, Theroux P, Solares J, Alonso J, Fernandez-Aviles F, Elizaga J, et al. Determinants of hemorrhagic infarcts. Histologic observations from experiments involving coronary occlusion, coronary reperfusion, and reocclusion. Am J Pathol 1990;137(2):301–11.
[79] Weis SM, Cheresh DA. Pathophysiological consequences of VEGF-induced vascular permeability. Nature 2005;437(7058):497–504.
[80] Feng Y, Venema VJ, Venema RC, Tsai N, Behzadian MA, Caldwell RB. VEGF-induced permeability increase is mediated by caveolae. Invest Ophthalmol Vis Sci 1999;40(1):157–67.
[81] Kloner RA, Ganote CE, Jennings RB. The “no-reflow” phenomenon after temporary coronary occlusion in the dog. J Clin Invest 1974;54(6):1496–508.
[82] Piper HM, Garcia-Dorado D. Prime causes of rapid cardiomyocyte death during reperfusion. Ann Thorac Surg 1999;68(5):1913–9.
[83] Ruiz-Meana M, Garcia-Dorado D, Gonzalez MA, Barrabes JA, Soler-Soler J. Effect of osmotic stress on sarcolemmal integrity of isolated cardiomyocytes following transient metabolic inhibition. Cardiovasc Res 1995;30(1):64–9.
[84] Nakamura H, Nemenoff RA, Gronich JH, Bonventre JV. Subcellular characteristics of phospholipase A2 activity in the rat kidney. Enhanced cytosolic, mitochondrial, and microsomal phospholipase A2 enzymatic activity after renal ischemia and reperfusion. J Clin Invest 1991;87(5):1810–8.
[85] Corr PB, Gross RW, Sobel BE. Amphipathic metabolites and membrane dysfunction in ischemic myocardium. Circ Res 1984;55(2):135–54.
[86] Inserte J, Garcia-Dorado D, Ruiz-Meana M, Agullo L, Pina P, Soler-Soler J. Ischemic preconditioning attenuates calpain-mediated degradation of structural proteins through a protein kinase A-dependent mechanism. Cardiovasc Res 2004;64(1):105–14.
[87] Inserte J, Garcia-Dorado D, Hernando V, Soler-Soler J. Calpain-mediated impairment of Na+/K+−ATPase activity during early reperfusion contributes to cell death after myocardial ischemia. Circ Res 2005;97(5):465–73.
[88] Inserte J, Garcia-Dorado D, Hernando V, Barba I, Soler-Soler J. Ischemic preconditioning prevents calpain-mediated impairment of Na+/K+−ATPase activity during early reperfusion. Cardiovasc Res 2006;70(2):364–73.
[89] Ruiz-Meana M, Inserte J, Fernandez-Sanz C, Hernando V, Miro-Casas E, Barba I, et al. The role of mitochondrial permeability transition in reperfusion-induced cardiomyocyte death depends on the duration of ischemia. Basic Res Cardiol 2011;106(6):1259–68.

[90] Bragadeesh T, Jayaweera AR, Pascotto M, Micari A, Le DE, Kramer CM, et al. Post-ischaemic myocardial dysfunction (stunning) results from myofibrillar oedema. Heart 2008;94(2):166–71.
[91] Vila-Petroff MG, Younes A, Egan J, Lakatta EG, Sollott SJ. Activation of distinct cAMP-dependent and cGMP-dependent pathways by nitric oxide in cardiac myocytes. Circ Res 1999;84(9):1020–31.
[92] Falck G, Schjott J, Jynge P. Hyperosmotic pretreatment reduces infarct size in the rat heart. Physiol Res 1999;48(5):331–40.
[93] Ganote CE, Worstell J, Iannotti JP, Kaltenbach JP. Cellular swelling and irreversible myocardial injury. Effects of polyethylene glycol and mannitol in perfused rat hearts. Am J Pathol 1977;88(1):95–118.
[94] Vander Heide RS, Sobotka PA, Ganote CE. Effects of the free radical scavenger DMTU and mannitol on the oxygen paradox in perfused rat hearts. J Mol Cell Cardiol 1987;19(6):615–25.
[95] Zhao ZQ, Corvera JS, Halkos ME, Kerendi F, Wang NP, Guyton RA, et al. Inhibition of myocardial injury by ischemic postconditioning during reperfusion: comparison with ischemic preconditioning. Am J Physiol Heart Circ Physiol 2003;285(2):H579–88.
[96] Bekkers SC, Yazdani SK, Virmani R, Waltenberger J. Microvascular obstruction: underlying pathophysiology and clinical diagnosis. J Am Coll Cardiol 2010;55(16):1649–60.
[97] Ochiai K, Shimada T, Murakami Y, Ishibashi Y, Sano K, Kitamura J, et al. Hemorrhagic myocardial infarction after coronary reperfusion detected in vivo by magnetic resonance imaging in humans: prevalence and clinical implications. J Cardiovasc Magn Reson 1999;1(3):247–56.
[98] Wu KC, Zerhouni EA, Judd RM, Lugo-Olivieri CH, Barouch LA, Schulman SP, et al. Prognostic significance of microvascular obstruction by magnetic resonance imaging in patients with acute myocardial infarction. Circulation 1998;97(8):765–72.
[99] Kloner RA, Rude RE, Carlson N, Maroko PR, DeBoer LW, Braunwald E. Ultrastructural evidence of microvascular damage and myocardial cell injury after coronary artery occlusion: which comes first? Circulation 1980;62(5):945–52.
[100] Sardella G, Mancone M, Canali E, Di Roma A, Benedetti G, Stio R, et al. Impact of thrombectomy with EXPort catheter in infarct-related artery during primary percutaneous coronary intervention (EXPIRA trial) on cardiac death. Am J Cardiol 2010;106(5):624–9.
[101] Sanz E, Garcia-Dorado D. Chronic heart failure (X). Ventricular remodelling in myocardial infarct. Rev Esp Cardiol 1992;45(6):397–411.
[102] Skrzypiec-Spring M, Grotthus B, Szelag A, Schulz R. Isolated heart perfusion according to Langendorff—still viable in the new millennium. J Pharmacol Toxicol Methods 2007;55(2):113–26.
[103] Garcia-Dorado D, Oliveras J, Gili J, Sanz E, Perez-Villa F, Barrabes J, et al. Analysis of myocardial oedema by magnetic resonance imaging early after coronary artery occlusion with or without reperfusion. Cardiovasc Res 1993;27(8):1462–9.
[104] Ghugre NR, Ramanan V, Pop M, Yang Y, Barry J, Qiang B, et al. Quantitative tracking of edema, hemorrhage, and microvascular obstruction in subacute myocardial infarction in a porcine model by MRI. Magn Reson Med 2011;66(4):1129–41.
[105] Monmeneu JV, Bodi V, Sanchis J, Lopez-Lereu MP, Mainar L, Nunez J, et al. Cardiac magnetic resonance evaluation of edema after ST-elevation acute myocardial infarction. Rev Esp Cardiol 2009;62(8):858–66.
[106] Eitel I, Knobelsdorff-Brenkenhoff F, Bernhardt P, Carbone I, Muellerleile K, Aldrovandi A, et al. Clinical characteristics and cardiovascular magnetic resonance findings in stress (takotsubo) cardiomyopathy. JAMA 2011;306(3):277–86.
[107] Chitwood Jr WR, Sink JD, Hill RC, Wechsler AS, Sabiston Jr DC. The effects of hypothermia on myocardial oxygen consumption and transmural coronary blood flow in the potassium-arrested heart. Ann Surg 1979;190(1):106–16.
[108] Ledingham SJ, Katayama O, Lachno DR, Yacoub M. Prolonged cardiac preservation. Evaluation of the University of Wisconsin preservation solution by comparison with the St. Thomas' Hospital cardioplegic solutions in the rat. Circulation 1990;82(5 Suppl):IV351–8.
[109] George TJ, Arnaoutakis GJ, Baumgartner WA, Shah AS, Conte JV. Organ storage with University of Wisconsin solution is associated with improved outcomes after orthotopic heart transplantation. J Heart Lung Transplant 2011;30(9):1033–43.
[110] Davis KL, Laine GA, Geissler HJ, Mehlhorn U, Brennan M, Allen SJ. Effects of myocardial edema on the development of myocardial interstitial fibrosis. Microcirculation 2000;7(4):269–80.
[111] Desai KV, Laine GA, Stewart RH, Cox Jr CS, Quick CM, Allen SJ, et al. Mechanics of the left ventricular myocardial interstitium: effects of acute and chronic myocardial edema. Am J Physiol Heart Circ Physiol 2008;294(6):H2428–34.
[112] Laine GA. Microvascular changes in the heart during chronic arterial hypertension. Circ Res 1988;62(5):953–60.
[113] Friedrich MG, Strohm O, Schulz-Menger J, Marciniak H, Luft FC, Dietz R. Contrast media-enhanced magnetic resonance imaging visualizes myocardial changes in the course of viral myocarditis. Circulation 1998;97(18):1802–9.
[114] Rottgen R, Christiani R, Freyhardt P, Gutberlet M, Schultheiss HP, Hamm B, et al. Magnetic resonance imaging findings in acute myocarditis and correlation with immunohistological parameters. Eur Radiol 2011;21(6):1259–66.
[115] Patel SM, Jameel F, Pikal MJ. The effect of dryer load on freeze drying process design. J Pharm Sci 2010;99(10):4363–79.
[116] Mehlhorn U, Allen SJ, Adams DL, Davis KL, Gogola GR, de Vivie ER, et al. Normothermic continuous antegrade blood cardioplegia does not prevent myocardial edema and cardiac dysfunction. Circulation 1995;92(7):1940–6.
[117] Abdallah Y, Kasseckert SA, Iraqi W, Said M, Shahzad T, Erdogan A, et al. Interplay between Ca2+ cycling and mitochondrial permeability transition pores promotes reperfusion-induced injury of cardiac myocytes. J Cell Mol Med 2011;15(11):2478–85.
[118] Capo-Aponte JE, Iserovich P, Reinach PS. Characterization of regulatory volume behavior by fluorescence quenching in human corneal epithelial cells. J Membr Biol 2005;207(1):11–22.
[119] Roos KP. Length, width, and volume changes in osmotically stressed myocytes. Am J Physiol 1986;251(6 Pt 2):H1373–8.
[120] Diaz RJ, Armstrong SC, Batthish M, Backx PH, Ganote CE, Wilson GJ. Enhanced cell volume regulation: a key protective mechanism of ischemic preconditioning in rabbit ventricular myocytes. J Mol Cell Cardiol 2003;35(1):45–58.
[121] Aliev MK, Khatkevich AN, Tsyplenkova VG, Meertsuk FE, Kapelko VI. Tracer kinetics analysis of the extracellular spaces in saline perfused hearts. Exp Clin Cardiol 2001;6(4):188–94.
[122] Olivetti G, Anversa P, Loud AV. Morphometric study of early postnatal development in the left and right ventricular myocardium of the rat. II. Tissue composition, capillary growth, and sarcoplasmic alterations. Circ Res 1980;46(4):503–12.
[123] Grochowski EC, Ganote CE, Hill ML, Jennings RB. Experimental myocardial ischemic injury. I. A comparison of Stadie-Riggs and free-hand slicing techniques on tissue ultrastructure, water and electrolytes during in vitro incubation. J Mol Cell Cardiol 1976;8(3):173–87.
[124] Friedrich MG. Myocardial edema—a new clinical entity? Nat Rev Cardiol 2010;7(5):292–6.
[125] Le Bihan D, Breton E, Lallemand D, Grenier P, Cabanis E, Laval-Jeantet M. MR imaging of intravoxel incoherent motions: application to diffusion and perfusion in neurologic disorders. Radiology 1986;161(2):401–7.
[126] Rapacchi S, Wen H, Viallon M, Grenier D, Kellman P, Croisille P, et al. Low b-value diffusion-weighted cardiac magnetic resonance imaging: initial results in humans using an optimal time-window imaging approach. Invest Radiol 2011;46(12):751–8.
[127] Kiricuta Jr IC, Simplaceanu V. Tissue water content and nuclear magnetic resonance in normal and tumor tissues. Cancer Res 1975;35(5):1164–7.
[128] Aletras AH, Tilak GS, Natanzon A, Hsu LY, Gonzalez FM, Hoyt Jr RF, et al. Retrospective determination of the area at risk for reperfused acute myocardial infarction with T2-weighted cardiac magnetic resonance imaging: histopathological and displacement encoding with stimulated echoes (DENSE) functional validations. Circulation 2006;113(15):1865–70.
[129] Friedrich MG, Abdel-Aty H, Taylor A, Schulz-Menger J, Messroghli D, Dietz R. The salvaged area at risk in reperfused acute myocardial infarction as visualized by cardiovascular magnetic resonance. J Am Coll Cardiol 2008;51(16):1581–7.
[130] Simonetti OP, Kim RJ, Fieno DS, Hillenbrand HB, Wu E, Bundy JM, et al. An improved MR imaging technique for the visualization of myocardial infarction. Radiology 2001;218(1):215–23.
[131] Axel L. Blood flow effects in magnetic resonance imaging. AJR Am J Roentgenol 1984;143(6):1157–66.

ORIGINAL RESEARCH

American Heart Association | American Stroke Association

Measuring Water Distribution in the Heart: Preventing Edema Reduces Ischemia–Reperfusion Injury

Mireia Andrés-Villarreal, MD; Ignasi Barba, PhD; Marcos Poncelas, PhD; Javier Inserte, PhD; José Rodriguez-Palomares, MD, PhD; Victor Pineda, MD, PhD; David Garcia-Dorado, MD, PhD, FAHA

***Background*—**Edema is present in many heart diseases, and differentiation between intracellular (ICW) and extracellular (ECW) myocardial water compartments would be clinically relevant. In this work we developed a magnetic resonance imaging–based method to differentiate ICW and ECW and applied it to analyze ischemia–reperfusion–induced edema.

***Methods and Results*—**Isolated rat hearts were perfused with gadolinium chelates as a marker of extracellular space. Total water content was measured by desiccation. Gadolinium quantification provided ECW, and ICW was calculated by subtraction of ECW from total water content. In separate experiments, T1, T2, diffusion-weighted imaging and proton-density parameters were measured in isolated saline-perfused hearts. In in-situ rat hearts, ECW and ICW were 79±10 mL and 257±8 mL of water per 100 g of dry tissue, respectively. After perfusion for 40 minutes, ECW increased by 92.4±3% without modifying ICW (−1±3%). Hyposmotic buffer (248 mOsm/L) increased ICW by 16.7±2%, while hyperosmotic perfusion (409 mOsm/L) reduced ICW by 26.5±3%. Preclinical imaging showed good correlation between T2 and diffusion-weighted imaging with ECW, and proton-density correlated with total water content. Ischemia–reperfusion resulted in marked myocardial edema at the expense of ECW, because of cellular membrane rupture. When cell death was prevented by blebbistatin, water content and distribution were similar to normoxic perfused hearts. Furthermore, attenuation of intracellular edema with hyperosmotic buffer reduced cell death.

***Conclusions*—**We devised a method to determine edema and tissue water distribution. This method allowed us to demonstrate a role of edema in reperfusion-induced cell death and could serve as a basis for the study of myocardial water distribution using magnetic resonance imaging. **(*J Am Heart Assoc*. 2016;5:e003843 doi: 10.1161/JAHA.116.003843)**

Key Words: edema • gadolinium chelates • hyperosmotic reperfusion • ischemia • magnetic resonance imaging

Myocardial edema appears in many heart diseases and pathologic situations involving the heart: ischemic syndromes,[1–3] cardiac inflammation (myocarditis and graft rejection),[4,5] and mechanical overload secondary to valve disease or arterial hypertension.[6,7] Acute myocardial infarction and apical ballooning syndrome are characterized by significant myocardial edema in the ischemic[8–10] or transiently dyskinetic segments.[1,11,12] Literature suggests that intracellular myocardial edema may have a role in cardiomyocyte cell death,[13] myocardial stunning,[14,15] and in the nonreflow phenomenon.[16–19] On the other hand, laboratory experiments suggest that interstitial edema secondary to pressure overload may be related to the genesis of myocardial fibrosis,[20] and to be one of the underlying mechanisms of diastolic dysfunction.[21,22]

Magnetic resonance imaging (MRI) consists of measuring protons and their properties in a 3-dimensional space and turning the information into images. Heart MRI signal comes mainly from water protons; thus, it is the method of choice for the study of edema. T1 values have been used to measure extracellular volume,[23] but the method requires some assumptions, such as a dynamic steady state for gadolinium (Gd)-containing extracellular marker that may not be adequate in certain pathological circumstances.

Edematous areas in the heart appear bright in T2-weighted images because the T2 relaxation time becomes longer.[11] T2-weighted cardiac MRI is increasingly being used in clinical practice as a diagnostic tool and also to retrospectively evaluate the area at risk (myocardium that suffered ischemia during transient coronary occlusion) as a variable to normalize infarct size limitation as a primary end point in clinical trials of

From the Cardiology Department, Vall d'Hebron University Hospital and Research Institute, Universitat Autònoma de Barcelona, Spain (M.A.-V., I.B., M.P., J.I., J.R.-P., D.G.-D.); Institut Diagnostic per la Imatge, Barcelona, Spain (M.A.-V., V.P.).

Correspondence to: Ignasi Barba, PhD, or David Garcia-Dorado, MD, PhD, FAHA, Cardiology Department, Hospital Vall d'Hebron, Passeig de la Vall d'Hebron 119, Barcelona 08035, Spain. E-mails: ignasi.barba@vhir.org; dgdorado@vhebron.net

Received May 4, 2016; accepted October 5, 2016.

reperfusion injury.[24] However, using T2-weighted images is subject to limitations including acquisition timing dependence of the results[25] and influence of treatments as pre-, post-, or remote ischemic conditioning.

Information regarding myocardial water distribution may shed light into the pathophysiology of various processes including reperfusion injury. However, current experimental methods to determine water distribution between intra- and extracellular tissue compartments are based on radionuclide labeling of macromolecules with suitable diffusion properties[8–10] that are difficult to translate to clinical practice.

In this study we devised a reliable method to determine myocardial water distribution using MRI, which could serve as a basis for the development of methods with clinical application, and applied it to investigate whether edema does contribute to cardiomyocyte death after ischemia–reperfusion (IR).

Table 1. Composition and Osmolarity for the Different Buffers Used in This Work

	Krebs Henseleit	Hyposmotic Modified KH	Hyperosmotic Modified KH
Osmolarity, mOsm/L	308	248	409
NaCl	118	88	118
KCl	4.7	4.7	4.7
Mg_2SO_4	1.2	1.2	1.2
$NaHCO_3$	25	25	25
$CaCl_2$	1.8	1.8	1.8
KH_2PO_4	1.2	1.2	1.2
Glucose	11	11	11
Mannitol			101

Units in mmol/L. KH indicates Krebs-Henseleit.

Methods

Animals

All the experiments were carried out with male Sprague-Dawley rats weighting 300 to 350 g. Animals were cared for according to the European laws and to the instructions provided in the "Guide for the Care and Use of Laboratory Animals" published by the US National Institutes of Health (NIH Publication No. 85-23, revised 1996). The experimental protocols were approved by the Animal Ethics Committee at "Vall d'Hebron Institut de Recerca."

In Situ Rat Heart Experiments

In situ experiments were performed in 4 animals. Anesthesia was induced with 5% isoflurane and maintained with isoflurane 2%. ECG and rectal temperature were continuously monitored during the experiment as well as appropriate anesthetic level. The jugular vein and the carotid artery were cannulated and a solution of gadobutrol 1 mmol/mL was perfused for 5 minutes at 0.35 μL/min per gram through the jugular vein. This perfusion rate was established in order to achieve a Gd plasma concentration between 1 and 10 mmol/L, assuming a blood volume of around 50 to 70 mL/kg and cardiac output 121 mL/kg per minute and a volume of distribution in steady state of 0.20 L/kg. A blood sample from the carotid artery was obtained during the last 30 s of Gd-BT-DO3A perfusion, just before the excision of the heart. The removed heart was washed in NaCl 0.9% at 4°C.

Saline-Perfused Isolated Rat Heart Experiments

Animals were anesthetized with an intraperitoneal pentobarbital overdose injection (100 mg/kg). Once deep unconsciousness was achieved, hearts were removed by a subxiphoidal incision and thoracotomy. Hearts were washed in cold (4°C) saline solution (NaCl 0.9%) and hung at the cannula of a continuous perfusion system through the ascending aorta. Hearts were retrogradely perfused with continuously oxygenated buffer at 37°C. Flow was adjusted to obtain a perfusion pressure between 45 and 60 mm Hg. A balloon was allocated at the left ventricle chamber and inflated to achieve 8 to 12 mm Hg of telediastolic pressure. Left ventricle developed pressure and perfusion pressure were monitored throughout the experiment.[26]

In order to evaluate the effects of different buffer osmolarities in water distribution during normoperfusion, we used 3 perfusion buffers with varying osmolarity to induce different patterns of water distribution between the intracellular and extracellular compartments. Control hearts (n=8) were perfused with Krebs-Henseleit buffer at 308 mOsm/L. Hyposmotic experiments (n=9) were conducted in low-NaCl to obtain an osmolarity of 248 mOsm/L, and mannitol (n=11) was added to obtain high osmolarity of 409 mOsm/L. In all cases pH was adjusted to 7.4 (see Table 1 for complete buffer composition).

In all cases, perfusion lasted for 40 minutes and during the last 5 minutes, Gd chelate (gadobutrol) was added to a final concentration of 1 mmol/L (Figure 1A); it was previously checked that after 3.5 minutes the concentration of Gd in the effluent achieved steady-state (data not shown).

I–R Protocols in the Crystalloid Perfused Isolated Rat Heart

Figure 1B shows the protocols designed to study the effects of edema in IR injury. The protocol included 30 minutes of perfusion (equilibration period) followed by 40 minutes of

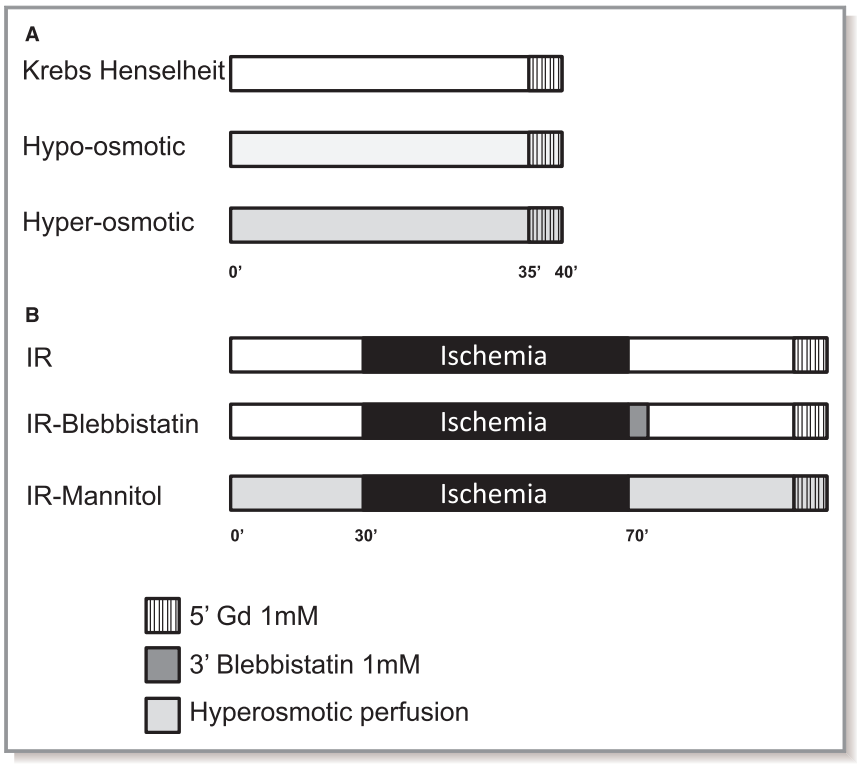

Figure 1. Perfusion protocols. A, Experiments with normoxic perfusion at different osmolarity: normosmotic Krebs-Henseleit (KH), hyposmotic low-NaCl modified KH and hyperosmotic mannitol modified KH. Gd was perfused during the last 5 minutes of perfusion. B, The perfusion protocols of the ischemia–reperfusion (IR) experiments: in all cases a 30-minute stabilization period preceded the 40 minutes of ischemia followed by 30 minutes of reperfusion. White bars correspond to Krebs Henseleit buffer; light gray, hyperosmotic buffer; dark gray to blebbistatin containing buffer and shadowed areas to gadolinium containing buffer. Samples for LDH quantification were taken during reperfusion. Blebbistatin was perfused during the first 3 minutes of reperfusion in the blebbistatin group. Hyperosmotic mannitol modified-KH buffer was perfused both during the stabilization period and reperfusion in the hyperosmotic IR group. In all cases 1 mmol/L Gd was added to the perfusion buffer during the last 5 minutes of reperfusion. LDH indicates lactate dehydrogenase.

ischemia at 37°C (perfusion discontinuation) and 30 minutes of reperfusion.

Three groups were analyzed: the control IR group with Krebs-Henseleit buffer (n=6), the blebbistatin-treated group (n=4), and the mannitol group (n=4). Blebbistatin prevents hypercontracture and cell death[27,28] and it has been used in this protocol to maintain intra- and extracellular space integrity by avoiding membrane rupture; blebbistatin was added during the first 3 minutes of reperfusion.[27]

Effluent samples were obtained during reperfusion to quantify infarct size by lactate-dehydrogenase (LDH) release. LDH is expressed as units 5 $min^{-1} \cdot g^{-1}$.

Measurement of Total Water Content

Once the hearts were removed from the perfusion system or, in the case of in situ experiments, washed in cold physiologic serum to remove excess blood, the surrounding excess water was carefully removed with the aid of a nylon membrane. Hearts were cut in 3 parts excluding the valve plane (apex and 2 symmetric sections of the basal portion, both containing similar amounts of right and left ventricle mass). Each portion was weighed and then freeze-dried overnight. After freeze-drying, samples were weighed again in order to obtain the dry mass. The difference between the fresh and the dry mass provided total water content (TWC) of each sample. Freeze-dried samples were stored at −20°C until Gd extraction.

Extracellular Water Content Measurement

Freeze-dried samples were micronized inside an assay tube using a spatula. Once micronized, 1 mL of miliQ water was added to the sample, vortex-shook, and let stand for 10 minutes at room temperature. Afterwards the sample

was centrifuged at 2000*g* for 5 minutes and the supernatant containing Gd was recovered. Only the first extraction was used for the final analysis, after checking that further extracts did not provide additional information about Gd content. Gd concentration in the effluent was measured at the time of heart removal in each experiment.

Gd measurement was based on the fact that Gd concentration proportionally shortens the spin-lattice relaxation time (T1).[29] To measure T1 in each sample, the extract was put into a 5-mm MR tube. Seven samples and 5 calibration line tubes (containing Gd at 0–0.5–0.6–0.8–1 mmol/mL) were allocated into the 40-mm MR coil for each measurement. Images were acquired in a vertical 9.4T magnet interfaced to a Bruker® (Madrid, Spain) Avance console. Sequence details: ET=4 ms, RT×9 (6.000–4.000–3.000–2.000–1.000–500–250–125–62.5) ms, where ET is echo time and RT repetition time matrix: 256×256-pixel resolution in a 30×30-mm window and slice thickness of 1.0 mm. For each sample, a region of interest at the center of the tube was obtained and the signal intensity was measured. This signal intensity was plotted against RT and fitted to an exponential function provided by Bruker software to obtain the T1 value. This function was used to calculate the concentration of Gd from measured T1 values.

In the case of the in situ experiments, Gd concentration in the animal serum was also analyzed. Arterial blood sample (0.3 mL) was obtained at the time of euthanizing and left to coagulate at room temperature. Afterwards the sample was centrifuged at 2000*g* for 10 minutes in order to obtain the serum, which was stored at −20°C until MR analysis.

MRI of Perfused and In Situ Hearts

In a separate set of experiments (n=4 for Krebs-Henseleit, hyposmotic, and hyperosmotic perfused groups), we measured T2, diffusion-weighted imaging, and proton-density values of rat hearts after saline perfusion without Gd. Nonperfused hearts (n=2) were removed from the animal and washed in cold physiologic serum before MRI measurements. T2 was measured with a spin-echo pulse sequence with a RT of 6000 ms and 16 echoes of 4 ms. Proton-density was defined as the voxel mean signal intensity of the first echo image obtained with a pulse-echo sequence with RT 10 000 ms and echo time of 4 ms and expressed as a percentage of the intensity of free water.

Diffusion-weighted images were acquired with a DtiEPI pulse sequence with ET set at 25 ms and RT at 3000 ms, and 7 b-values between 4 and 755 s/mm^2.

Infarct Size Measurement

In the isolated heart model, infarct size was estimated with the area under the curve of the LDH release during the reperfusion period as previously described.[30] LDH data are expressed as units of activity released per gram of dry weight during the first 5 minutes of reperfusion.

Statistical Analysis

Data were analyzed using ANOVA and Tukey's post hoc test by means of commonly available software (SPSS version 15 for Windows (SPSS Inc, Chicago, IL)). Correlation test was made by linear regression analysis using SigmaPlot software. Data were checked for normality using the Kolmogorov–Smirnov test. Differences with $P<0.05$ were considered statistically significant. Results are given as mean±SE.

Results

Heart hemodynamics during saline perfusion were similar between the different experimental protocols. IR induced extensive cell death (LDH: 353±67) in contrast to control perfusion (LDH: 56±16 $P<0.05$). Cell death was prevented by the use of blebbistatin during the first 3 minutes of reperfusion (LDH: 65±17, P=ns versus control).

$T1^{-1}$ and [Gd] showed a good linear correlation when [Gd] <5 mmol/L (r^2=0.997±0.0042; n=55 calibration curves), thus allowing adequate measurement of extracellular space. Correlation between LogT1 and [Gd] was linear for [Gd] <0.1 mmol/L.

Edema Distribution Studies

In situ hearts contained 336±5 mL water/100 g dry tissue, 257±8 mL/100 g of it were intracellular and the remaining 79±10 mL/100 g extracellular. Perfusion with Krebs-Henseleit buffer for 40 minutes induced edema (an increase of 19% of TWC) at the expense of extracellular myocardial water compartments (ECW) with preserved intracellular myocardial water compartments (ICW) content. In the normo-osmotic saline-perfused hearts, TWC was 406±6 mL/100 g ($P<0.001$), ECW 152±5 mL/100 g ($P<0.01$), and ICW 254±7 mL/100 g (P=ns versus in situ hearts).

Perfusion with hyposmotic buffer induced an additional 9% increase of TWC because of an 18% increase of the intracellular water compartment: TWC 444±2.6 mL/100 g ($P<0.01$), ECW 144±5.6 mL/100 g (P=ns), and ICW 300±5 mL/100 g ($P<0.01$). On the other hand, hyperosmotic perfusion decreased TWC by 10% at the expense solely of the ICW compartment (reduced by 26%): TWC 362±4.4 mL/100 g ($P<0.01$), ECW 172±6.5 mL/100 g (P=ns), and ICW 189±5.3 mL/100 g ($P<0.01$), suggesting water redistribution from the ICW space to the interstitium. All saline-perfused groups showed a significant increase of ECW as compared to in vivo hearts ($P<0.01$) but did not show significant differences

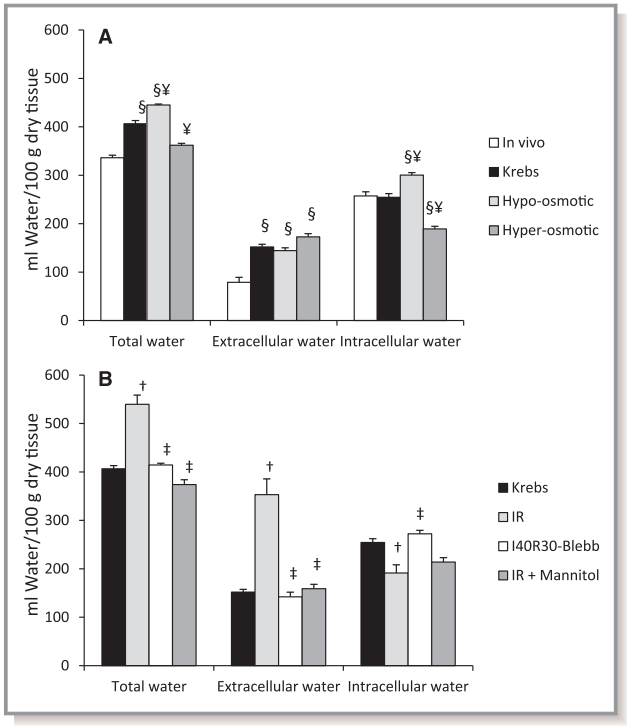

Figure 2. Myocardial water content and distribution. A, Water content (mL/100 g dry tissue) in the in situ (n=4) and normoxic perfused hearts (control Krebs-Henseleit [KH] n=8; hyposmotic n=9, hyperosmotic n=11). $^{\S}P<0.05$ compared to nonperfused (in situ) heart. $^{¥}P<0.05$ compared to KH perfused hearts. B, Ischemia–reperfusion insulted hearts (IR group n=6, IR blebbistatin group n=4; IR mannitol group n=4) compared to KH normoxic perfused hearts. $^{\dagger}P<0.05$ compared to KH perfused hearts. $^{\ddagger}P<0.05$ compared to IR insulted hearts.

in ECW between them. Water content and distribution in the different groups is shown in Figure 2 and Table 2.

Hearts subjected to IR showed a marked increase in TWC in comparison to nonischemic saline-perfused hearts. The Gd-diffusible space (ECW) increased by 200 mL/100 g as

Table 2. Water Content and Distribution During the Different Protocols

	TWC	ECWC	ICWC
In situ	336±5	79±10	257±8
KH 40′	406±6	152±5	243±13
Hyposmotic 40′	445±2	144±6	306±8
Hyperosmotic 40′	361±4	172±7	189±5
IR	539±19	353±32	191±17
IR-blebbistatin	414±4	142±10	272±7
IR-hyperosmotic	374±10	159±9	214±9

All data are in mL of water per 100 g of dry tissue. Values are expressed as mean±SD. ECWC indicates extracellular water content; ICWC, intracellular water content; IR, ischemia–reperfusion injury protocols; KH, Krebs-Henseleit; TWC, total water content.

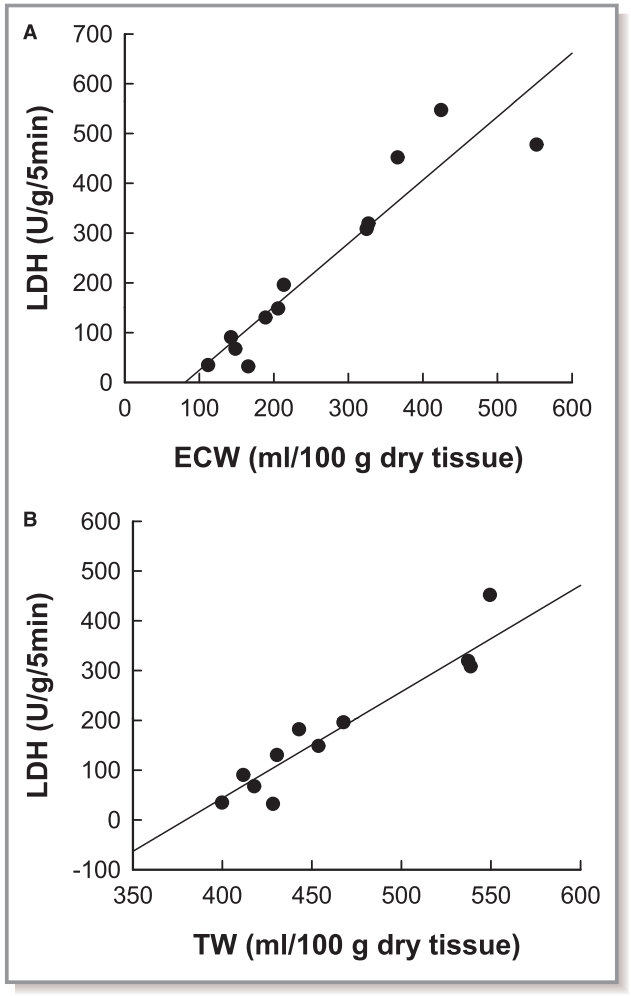

Figure 3. Graph showing the correlation between edema and cell death (n=12). A, Corresponds to the correlation between extracellular water and LDH while (B) shows total water content against cell death measured as LDH release. ECW indicates extracellular water; LDH, lactate dehydrogenase; TW, total water.

compared to control perfused hearts; however, ICW was reduced after IR (Figure 2B). Total and extracellular water compartments showed a good linear correlation with the extent of cell death after IR injury measured as LDH release (r^2=0.9485, $P<0.01$, and r^2=0.8844, $P<0.01$, respectively) as shown in Figure 3.

Preventing hypercontracture with blebbistatin markedly attenuated cell death induced by IR (LDH 353±67 versus 65±17, $P<0.05$) and edema (539±18 versus 414±4 mL/100 g, $P<0.05$) (Table 2). Likewise, reducing intracellular edema with the use of a hyperosmotic buffer prevented cell death (LDH 36±15; P=ns versus control).

MRI of Perfused and In Situ Hearts

In a separate set of experiments, we obtained MR images of the in situ and saline-perfused hearts under different osmotic

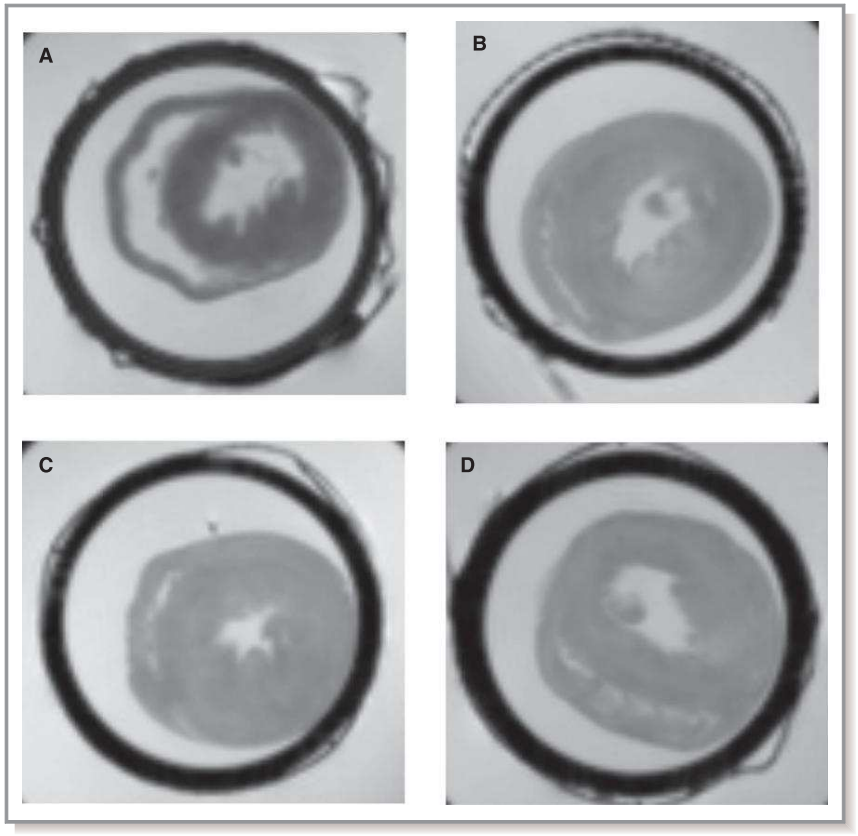

Figure 4. Ex-vivo images of rat hearts acquired with a RARE pulse sequence, TR 10 000 and TE 13 ms. A, Corresponds to a nonperfused heart, (B through D) to hearts perfused in the Langendorff system with hyperosmotic, normo-osmotic and hypo-osmotic buffers, respectively. Note that perfusion induces a high degree of edema. Hearts appear in black circles that correspond to plastic tubing used to center the organs. RARE indicates rapid acquisition with relaxation enhancement.

stress conditions (Figure 4), and found that T2 values showed good correlation with extracellular water content (r^2=0.993, P<0.01) while proton-density values correlated with total water content (r^2=0.988, P<0.01). On the other hand, T2 and proton-density showed poor correlation with total and extracellular water content, respectively (r^2=0.305 and 0.318, p=ns) (Figure 5). The diffusion-weighted imaging constant also showed a correlation with ECW although not as strong as T2 (r^2=0.893, P<0.01).

Discussion

In this work we presented a method based on extracellular space labeling using Gd that allows determination of water distribution in the myocardium. In this context, extracellular water is equivalent to the Gd diffusible space that includes intravascular and interstitial spaces. The method provided physiologically meaningful data on the effect of IR on intra- and extracellular water distribution. Comparison of the results obtained with this method with MRI variables indicates that T2 correlated with EWC while total water content correlated with proton-density. Data presented here support the notion that intracellular edema may contribute to cardiomyocyte death during initial reperfusion.

At present there is no "gold standard" to measure water content and distribution, but our measures based on Gd-chelates in intact heart are in close agreement with previous work done using radionuclide-labeled compounds.[31] The results presented here for in situ experiments are in close agreement with the literature data showing ECW values between 69 and 112 (mean value 95) mL/100 g dry tissue and ICW between 263 and 278 (mean value 271) mL/100 g dry tissue.[31] TWC in Langendorff-perfused rat hearts ranged from 429 to 784 mL/100 g dry tissue; ECW from 175 to 603 (mean value of 374) mL/100 g dry tissue, and ICW ranged from 181 to 253 (mean value of 224) mL/100 g dry tissue.[31] The highest variability was found in ECW content. One of the reasons leading to this great variability could be the removal of the buffer surrounding the heart; we found that this step is crucial in obtaining accurate and reproducible results.

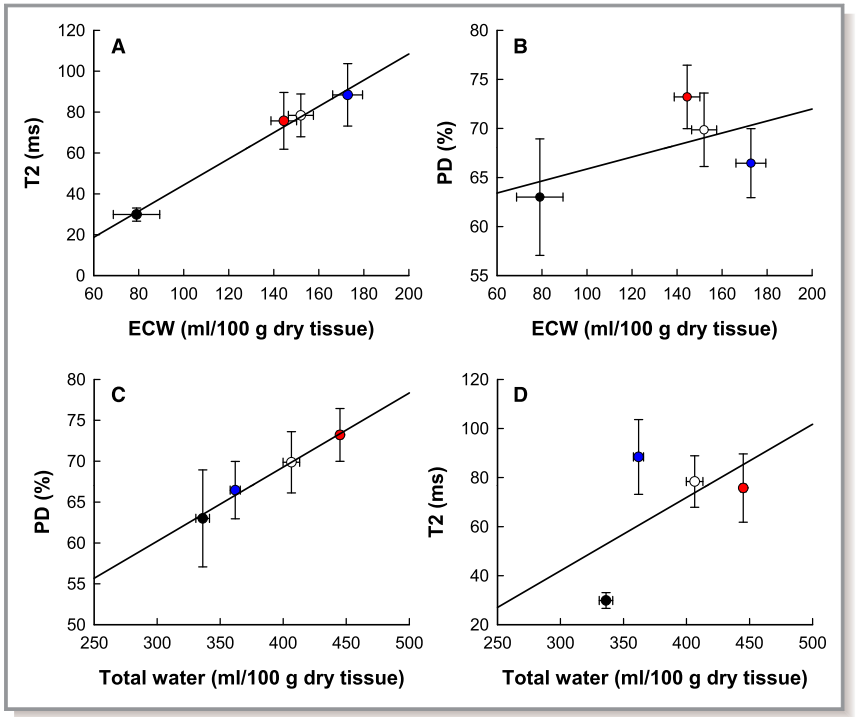

Figure 5. Correlation between MRI parameters and edema components (A) shows a good correlation between T2 and extracellular water while (B) shows that ECW does not correlate with proton-density. C, Corresponds to the correlation between proton-density and total water content and (D) is the correlation between proton-density and extracellular water. Black symbols correspond to in situ experiments, red to hypo-osmotic perfusion, white to normo-osmotic, and blue to hyper-osmotic perfusion protocols. Each point is the average of various experiments (n=4 each for MRI experiments, except for nonperfused group with n=2; n=4, 8, 9, 11 for in situ, control, hyposmotic, and hyperosmotic groups, respectively in the water content experiments; error bars show SE).

Early cell death during reperfusion occurs mainly through necrosis involving sarcolemmal rupture.[32] Our results show that intracellular space diminishes inversely proportional to IR injury, which is consistent with sarcolemmal rupture and intracellular space becoming accessible to Gd chelates. Prevention of cardiomyocyte death with myosin–actin inhibitors—both 2,3-butanedione monoxime[33,34] and the more specific blebbistatin[28]—also prevented intracellular space from becoming extracellular, proving that, at least part, the increase of extracellular edema is due to sarcolemmal rupture and Gd chelates having access to that space.

The contribution of reperfusion-induced cellular edema to cell death and myocardial infarct size was suggested over 2 decades ago[24] but has been a subject of controversy,[35] in part due to the lack of confirmation regarding the effects of hyperosmotic reperfusion on intra- and extracellular edema. In the present study we have been able to show that when ICW edema is selectively prevented with a hyperosmotic medium, sarcolemmal rupture and infarct size are reduced in isolated perfused hearts. The present findings clearly support a role for edema as a mechanism of cell death during IR injury.

Our ex-vivo imaging results showed a good correlation between T2 and, to a lesser extent, apparent diffusion-weighted imaging coefficient, with extracellular water. Proton-density correlated with total water content, pointing towards the possibility of measuring myocardial water distribution through MRI and to the application of this method in patients.

Previous reports have described a correlation between T2 and total water content in IR models.[32,36] After extensive myocardial infarction, cell membranes lose their integrity, and intra- and extracellular water compartments mix. In these circumstances T2 would also correlate with total water content. On the other hand, the present experimental approach does allow modifying water distribution and we are able to prevent cell membrane rupture; the increase in number of conditions studied allowed us to correlate T2 with extracellular water.

Conclusions

In conclusion, we describe a method to measure myocardial edema distribution using MRI based on the kinetics and

magnetic properties of Gd chelates. This technique may be very useful in preclinical studies and could serve as a basis for the development of methods for a better characterization of myocardial edema in clinical practice.

Sources of Funding

This work was supported by grants from the "Instituto de Salud Carlos III" (ISCIII) PI13/00398 and RD12/42/21. M.A.-V. received a fellowship from ISCIII, FI12/00411.

Disclosures

None.

References

1. Abdel-Aty H, Cocker M, Friedrich MG. Myocardial edema is a feature of Tako-Tsubo cardiomyopathy and is related to the severity of systolic dysfunction: insights from T2-weighted cardiovascular magnetic resonance. *Int J Cardiol*. 2009;132:291–293.
2. Abdel-Aty H, Cocker M, Meek C, Tyberg JV, Friedrich MG. Edema as a very early marker for acute myocardial ischemia: a cardiovascular magnetic resonance study. *J Am Coll Cardiol*. 2009;53:1194–1201.
3. Berry C, Kellman P, Mancini C, Chen MY, Bandettini WP, Lowrey T, Hsu L-Y, Aletras AH, Arai AE. Magnetic resonance imaging delineates the ischemic area at risk and myocardial salvage in patients with acute myocardial infarction. *Circ Cardiovasc Imaging*. 2010;3:527–535.
4. Puntmann VO, Taylor PC, Barr A, Schnackenburg B, Jahnke C, Paetsch I. Towards understanding the phenotypes of myocardial involvement in the presence of self-limiting and sustained systemic inflammation: a magnetic resonance imaging study. *Rheumatology (Oxford)*. 2010;49:528–535.
5. Sasaguri S, Sunamori M, Saito K, Suzuki A. Early change of myocardial water during acute cardiac allograft rejection. *Jpn Circ J*. 1986;50:1113–1119.
6. Davis KL, Mehlhorn U, Laine GA, Allen SJ. Myocardial edema, left ventricular function, and pulmonary hypertension. *J Appl Physiol*. 1995;78:132–137.
7. Mehlhorn U, Davis KL, Laine GA, Geissler HJ, Allen SJ. Myocardial fluid balance in acute hypertension. *Microcirculation*. 1996;3:371–378.
8. Aliev MK, Khatkevich AN, Tsyplenkova VG, Meertsuk FE, Kapelko VI. Tracer kinetics analysis of the extracellular spaces in saline perfused hearts. *Exp Clin Cardiol*. 2001;6:188–194.
9. Askenasy N, Tassini M, Vivi A, Navon G. Intracellular volume measurement and detection of edema: multinuclear NMR studies of intact rat hearts during normothermic ischemia. *Magn Reson Med*. 1995;33:515–520.
10. Askenasy N, Navon G. Measurements of intracellular volumes by 59Co and 2H/1H NMR and their physiological applications. *NMR Biomed*. 2005;18:104–110.
11. Eitel I, von Knobelsdorff-Brenkenhoff F, Bernhardt P, Carbone I, Muellerleile K, Aldrovandi A, Francone M, Desch S, Gutberlet M, Strohm O, Schuler G, Schulz-Menger J, Thiele H, Friedrich MG. Clinical characteristics and cardiovascular magnetic resonance findings in stress (takotsubo) cardiomyopathy. *JAMA*. 2011;306:277–286.
12. Joshi SB, Chao T, Herzka DA, Zeman PR, Cooper HA, Lindsay J, Fuisz AR. Cardiovascular magnetic resonance T2 signal abnormalities in left ventricular ballooning syndrome. *Int J Cardiovasc Imaging*. 2010;26:227–232.
13. Garcia-Dorado D, Théroux P, Munoz R, Alonso J, Elizaga J, Fernandez-Avilés F, Botas J, Solares J, Soriano J, Duran JM. Favorable effects of hyperosmotic reperfusion on myocardial edema and infarct size. *Am J Physiol*. 1992;262:H17–H22.
14. Bragadeesh T, Jayaweera AR, Pascotto M, Micari A, Le DE, Kramer CM, Epstein FH, Kaul S. Post-ischaemic myocardial dysfunction (stunning) results from myofibrillar oedema. *Heart*. 2008;94:166–171.
15. Butler TL, Egan JR, Graf FG, Au CG, McMahon AC, North KN, Winlaw DS. Dysfunction induced by ischemia versus edema: does edema matter? *J Thorac Cardiovasc Surg*. 2009;138:141–147.
16. Kloner RA, Ganote CE, Jennings RB. The 'no-reflow' phenomenon after temporary coronary occlusion in the dog. *J Clin Invest*. 1974;54:1496–1508.
17. Bekkers SCAM, Yazdani SK, Virmani R, Waltenberger J. Microvascular obstruction: underlying pathophysiology and clinical diagnosis. *J Am Coll Cardiol*. 2010;55:1649–1660.
18. Reffelmann T, Kloner RA. The no-reflow phenomenon: a basic mechanism of myocardial ischemia and reperfusion. *Basic Res Cardiol*. 2006;101:359–372.
19. Tranum-Jensen J, Janse MJ, Fiolet WT, Krieger WJ, D'Alnoncourt CN, Durrer D. Tissue osmolality, cell swelling, and reperfusion in acute regional myocardial ischemia in the isolated porcine heart. *Circ Res*. 1981;49:364–381.
20. Davis KL, Laine GA, Geissler HJ, Mehlhorn U, Brennan M, Allen SJ. Effects of myocardial edema on the development of myocardial interstitial fibrosis. *Microcirculation*. 2000;7:269–280.
21. Sugihara N, Genda A, Shimizu M, Suematu T, Kita Y, Horita Y, Takeda R. Quantitation of myocardial fibrosis and its relation to function in essential hypertension and hypertrophic cardiomyopathy. *Clin Cardiol*. 1988;11:771–778.
22. Ohsato K, Shimizu M, Sugihara N, Konishi K, Takeda R. Histopathological factors related to diastolic function in myocardial hypertrophy. *Jpn Circ J*. 1992;56:325–333.
23. Kellman P, Wilson JR, Xue H, Ugander M, Arai AE. Extracellular volume fraction mapping in the myocardium, part 1: evaluation of an automated method. *J Cardiovasc Magn Reson*. 2012;14:63.
24. Garcia-Dorado D, Oliveras J. Myocardial oedema: a preventable cause of reperfusion injury? *Cardiovasc Res*. 1993;27:1555–1563.
25. Fernández-Jiménez R, Sánchez-González J, Agüero J, García-Prieto J, López-Martín GJ, García-Ruiz JM, Molina-Iracheta A, Rosselló X, Fernández-Friera L, Pizarro G, García-Álvarez A, Dall'Armellina E, Macaya C, Choudhury RP, Fuster V, Ibáñez B. Myocardial edema after ischemia/reperfusion is not stable and follows a bimodal pattern: imaging and histological tissue characterization. *J Am Coll Cardiol*. 2015;65:315–323.
26. Inserte J, Garcia-Dorado D, Ruiz-Meana M, Solares J, Soler J. The role of Na+-H+ exchange occurring during hypoxia in the genesis of reoxygenation-induced myocardial oedema. *J Mol Cell Cardiol*. 1997;29:1167–1175.
27. Inserte J, Hernando V, Vilardosa Ú, Abad E, Poncelas-Nozal M, Garcia-Dorado D. Activation of cGMP/protein kinase G pathway in postconditioned myocardium depends on reduced oxidative stress and preserved endothelial nitric oxide synthase coupling. *J Am Heart Assoc*. 2013;2:e005975 doi: 10.1161/JAHA.112.005975.
28. Dou Y, Arlock P, Arner A. Blebbistatin specifically inhibits actin-myosin interaction in mouse cardiac muscle. *Am J Physiol Cell Physiol*. 2007;293:C1148–C1153.
29. Weinmann H, Brasch R, Press W, Wesbey G. Characteristics of gadolinium-DTPA complex: a potential NMR contrast agent. *Am J Roentgenol*. 1984;142:619–624.
30. Rodríguez-Sinovas A, García-Dorado D, Ruiz-Meana M, Soler-Soler J. Protective effect of gap junction uncouplers given during hypoxia against reoxygenation injury in isolated rat hearts. *Am J Physiol Heart Circ Physiol*. 2006;290:H648–H656.
31. Aliev MK, Dos Santos P, Hoerter JA, Soboll S, Tikhonov AN, Saks VA. Water content and its intracellular distribution in intact and saline perfused rat hearts revisited. *Cardiovasc Res*. 2002;53:48–58.
32. García-Dorado D, Oliveras J, Gili J, Sanz E, Pérez-Villa F, Barrabés J, Carreras MJ, Solares J, Soler-Soler J, Garcia-dorado D, Oliveras J, Gili J, Sanz E, Perez-villa F, Barrabks J, Carreras MJ, Solares J. Analysis of myocardial oedema by magnetic resonance imaging early after coronary artery occlusion with or without reperfusion. *Cardiovasc Res*. 1993;27:1462–1469.
33. Li T, Sperelakis N, Teneick RE, Solaro RJ. Effects of diacetyl monoxime on cardiac excitation-contraction coupling. *J Pharmacol Exp Ther*. 1985;232:688–695.
34. Garcia-Dorado D, Théroux P, Duran JM, Solares J, Alonso J, Sanz E, Munoz R, Elizaga J, Botas J, Fernandez-Avilés F. Selective inhibition of the contractile apparatus. A new approach to modification of infarct size, infarct composition, and infarct geometry during coronary artery occlusion and reperfusion. *Circulation*. 1992;85:1160–1174.
35. Garcia-Dorado D, Andres-Villarreal M, Ruiz-Meana M, Inserte J, Barba I. Myocardial edema: a translational view. *J Mol Cell Cardiol*. 2012;52:931–939.
36. Fernández-jiménez R, Sánchez-gonzález J, Aguero J, Trigo M, Galán-arriola C, Fuster V, Ibáñez B. Fast T2 gradient-spin-echo (T2-GraSE) mapping for myocardial edema quantification: first in vivo validation in a porcine model of ischemia/reperfusion. *J Cardiovasc Magn Reson*. 2015;17:92. DOI 10.1186/s12968-015-0199-9